2D-REMPI of CF_3Br: Spectroscopy and Dynamics

Kári Sveinbjörnsson

Faculty of Physical Sciences
University of Iceland
2010

2D-REMPI of CF_3Br: Spectroscopy and Dynamics

Kári Sveinbjörnsson

16 ECTS thesis as a part of
Baccalaureus Scientiarum degree in Chemistry

Supervisors:
Prof. Ágúst Kvaran
Gísli Hólmar Jóhannesson, Ph.D.

Faculty of Physical Sciences
School of Engineering and Natural Sciences
University of Iceland
Reykjavík, December 2010

2D-REMPI of CF_3Br: Spectroscopy and dynamics
16 ECTS thesis as a part of *Baccalaureus Scientiarum* degree in Chemistry

Faculty of Physical Sciences
School of Engineering and Natural Sciences
University of Iceland
VRII, Hjarðarhagi 2-6
107 Reykjavík

Telephone: 525 4000

Registration information:
Kári Sveinbjörnsson, 2010, *2D-REMPI of CF_3Br: Spectroscopy and dynamics*, BS thesis, Faculty of Physical Sciences, University of Iceland, 42 bls.

ISBN:

Print:
Reykjavík, Janúar 2011

Hér með lýsi ég því yfir að ritgerð þessi er samin af mér og að hún hefur hvorki að hluta né í heild verið lögð fram áður til hærri prófgráðu.

I hereby declare that this report is written by me and has not been handed in at part or in whole for a higher education degree.

_____

Kári Sveinbjörnsson

Útdráttur

(2+n) REMPI litróf af CF_3Br fyrir jónirnar CF_3^+ og $^iBr^+$ (i = 79, 81) var skráð fyrir örvunarorkurnar 71 320 – 84 600 cm^{-1}. 1D-REMPI litróf fyrir mældu jónabrotin var svo fengið með því að heilda 2D-REMPI litrófið sem fékkst úr mælingunum. Einungis sáust merki fyrir CF_3^+, C^+ og $^{79,81}Br^+$ á þessu svæði og síðari tvö merkin voru ósamfelld og gáfu einungis skarpar atómlínur. Kolefnis og bróm atómlínurnar voru bornar saman við viðurkennd gildi úr NIST atómlínu gagnabankanum og var mismunurinn á milli atómlína þar sem hann var mestur rúm 0.01 %. Merkið frá CF_3^+ sást einungis fyrir þær örvunarorkur þar sem CF_3Br sameindin var örvuð á $[X^2E]$ 5p Rydberg ástand af frá grunnástandi. Færslur 4p $\rightarrow$ 5s sáust ekki vegna lítilla færslulíkinda þar sem færslan fylgir ekki valreglunni fyrir tveggja-ljóseinda örvun: $\Delta l = 0, \pm 2$.

Samfellt CF_3^+ merki og sterkar bróm atómlínur gefa til kynna að aðal ljósklofnunar ferill CF_3Br sé brot á C-Br tenginu og myndun CF_3 + Br stakeinda í gegnum fráhrindandi ástand. Klofnun í gegnum jónpara ástand sást einnig, auk myndunar á flúrljómandi CF_3* sameind. Aflháðar mælingar voru gerðar fyrir CF_3^+ merkið sem staðfestu að það var tilkomið vegna klofnunar í gegnum jónpara ástand.

Abstract

(2+n) REMPI spectra of CF_3Br for the ions CF_3^+ and $^iBr^+$ (i = 79, 81) was recorded for the excitation energy region 71 320 – 84 600 cm^{-1}. 1D-REMPI spectra for the measured ion fragments were constructed by integrating the 2D-REMPI spectra obtained from the measurements. Only CF_3^+, C^+ and $^{79,81}Br^+$ signals were observed during the measurements. The latter two ion fragment signals being non-continuous yielding only sharp atomic line peaks. The carbon and bromine atomic lines were compared to the NIST atomic line database and showed good agreement with the accepted values with a maximum error of about 0.01 %. The signal from CF_3^+ was only observed in the excitation energy region where the CF_3Br molecule was excited to a $[X^2E]$ 5p Rydberg state from a ground state. Transitions 4p $\rightarrow$ 5s were not observed due to the low transition probability since the transition does not follow the selection rule for two-photon excitation: $\Delta l = 0, \pm 2$.

Continuous CF_3^+ signal and strong bromine atomic lines would indicate that the major photodissociation mechanism of CF_3Br is breaking of the C-Br bond and the formation of CF_3 + Br radicals via a repulsive state. Dissociation via ion-pair state was observed aswell as the formation of a fluorescent CF_3* species. Power dependence measurements were done on the CF_3^+ signals which confirmed that the signal observed was from CF_3^+ formed via ion-pair state dissociation.

Index

Figure index

Table index

Acronyms

REMPI: Resonance Enhanced Multi-Photon Ionization

TOF: Time Of Flight

MS: Mass Spectrometry

BBO: Beta barium borate

MCP: Micro-channel plate

VUV: Visible & Ultra-Violet

NIST: National Institute of Standards and Technology

Acknowledgments

This research could not have been done without the invaluable support of Professor Ágúst Kvaran, Victor Huasheng Wang and Yingming Long. I would also like to thank Gísli Hólmar Jóhannesson, Ph.D. for support on reviewing and auditing the thesis.

1 Introduction

Over the past few decades spectroscopy and photofragmentation of freons has received considerable interest. Freons are volatile organic chemical compounds that contain carbon, halogens (chloride, bromide, iodide etc.) and fluorine and are derivatives of either methane or ethane. These compounds are widely used, mainly in industry, as refrigerants, propellants and solvents. It should not come as a surprise that freons are very efficient ozone depletion[1] chemicals and therefore play an important role in the atmosphere‘s chemistry. This ozone depletion element of the freons stems from the photodissociation of the chemical when it is bombarded by the ultra-violet radiation from the sun which forms a halide radical (fluorine, chlorine, bromine or iodine). That radical quickly attacks a nearby ozone molecule, when in the stratosphere, destroying it in the process. This can lead to an increase in UV radiation on Earth‘s surface which is harmful to life and is thought to be one of many causes of global warming. In this research the freon of interest is CF_3Br which was mostly used as a fire suppressant and a refrigerant until it was banned. Common alternative names include Halon 1301 and R13B1.

The Resonance Enhanced Multi-Photon Ionization (REMPI) method is used to measure the excited states in this study. It involves using one or more photons to excite a molecule to an electronically excited state from which the molecule either dissociates or remains intact and the fragments are then ionized with additional photons. A certain nomenclature, *(m+n)* REMPI, is used for the method describing how many photons are absorbed by the chemical of interest. The variable *m* describes the number of photons needed to perform resonance excitation of the molecule and the variable *n* describes the number of photons required to ionize the molecule or its fragments after excitation. In this research *(2+n)* REMPI is being observed, meaning that two photons are required to perform resonance excitation of the CF_3Br molecule and an unknown and variable number of *n* photons are used to ionize the fragments depending on the dissociation pathway of the excited molecule. REMPI relates to conventional absorption measurements in a way that if there is no absorption then it follows that no ionization is taking place and if absorption is present a signal is observed. Therefore, *(2+n)* REMPI is somewhat like an indirect two-photon absorption measurement. The usage of REMPI allows different excitations as compared to one-photon absorption measurements since more photons are used to excite the molecule. Meaning that the selection rule for the orbital angular momentum quantum number, *l*, varies with the number of photons exciting the chemical and thus different excitations are observed with REMPI.

Research has been done on the photofragmentation and absorption of methyl halides such as CH_3Br [2,3], which resembles CF_3Br in structure – tetrahedal and in the C_{3v} point group, and the main dissociation mechanism was found to be $CH_3Br^* \rightarrow CH_3 + Br$ [2], in other words, pure breaking of the C-Br bond. Another dissociation mechanism would

[1] (Environmental Chemistry - 4th edition, 2008)
[2] (Two-Dimensional (2+n) REMPI of CH_3Br: Photodissociation Channels via Rydberg States, 2010)
[3] (Vacuum ultraviolet absorption spectra of the bromomethanes, 1975)

involve the formation of the ion-pair [$CH_3^+Br^-$] but no other photofragmentation channels have been reported so far. Medium strong carbon *(2+1)* REMPI signals have been observed[2] which indicate that CH_3Br dissociates to some extent to form H_2 + C + HBr fragments.

REMPI on CF_3Br has not received much study, if any at all, and therefore this research is somewhat groundbreaking. However, there have been published numerous papers on one-photon absorption, fragmentation and ionization of the freon[3,4,5,6]. These researches all agree that the majority of the excited CF_3Br*, via one-photon excitation, dissociates to form a CF_3 and Br radicals[4] which resembles the fragmentation of CH_3Br. The dissociation energy of the CF_3Br molecule to form CF_3 and Br is 24 035 cm^{-1} [4] compared to the same fragmentation of CH_3Br with a dissociation energy of 24 588 cm^{-1} [7].

A Rydberg state is an excited electronic state which is primarily composed of atomic orbitals with principal quantum numbers, *n*, greater than the ground state and the valence excited states. Three major Rydberg states were discovered via VUV photoabsorption of CF_3Br corresponding to the transitions $4p \rightarrow [X^2E]\ 5s$, $4p \rightarrow [X^2E]\ 5p$ and $4p \rightarrow [^2A_1]\ 5s$,[8] with energies 70 735 cm^{-1}, 76 542 cm^{-1} and 84 849 cm^{-1} respectively[5] where the $4p \rightarrow 5s$ transition peaks were found to be considerably more intense due to the selection rule $\Delta l = \pm 1$ for transition probabilities via one-photon excitation. The ionization potential of CF_3Br has been measured thoroughly[6] as 91 979 ± 113 cm^{-1}.

In this study the focus was set on using REMPI to measure and study the photodissociation of CF_3Br at around the same excitation energy region as the transitions to the three major Rydberg states have been observed. The information obtained was then used to determine the photodissociation mechanism of CF_3Br, which could give further insight into the decomposition mechanism of ozone in the stratosphere.

---

[4] (Emission spectra of CF_3 radicals. V. Photodissociation of CF_3H, CF_3Cl, and CF_3Br by vacuum ultraviolet, 1983)
[5] (VUV photoabsorption in CF_3X (X = Cl, Br, I) fluoro-alkanes, 2006)
[6] (Photoionization of gas-phase bromotrifluoromethane and its complexes with methanol: State dependence of intracluster reactions, 1994)
[7] (Handbook of bond dissociation energies in organic compounds, 2003)
[8] (Electron impact excitation and dissociation of halogen-containing molecules, 2003)

2 Experimental Setup and Procedure

Measurements were performed using a tunable excitation radiation which was generated by Excimer laser-pumped dye laser system. The beam originated from a Lambda Physik COMPex 205 Excimer laser and passed through a Coherent ScanMatePro dye laser at a typical repetition rate of 10 Hz. Dyes C480, C503 and C540A were used and also dye R590 to some extent, although measurements with that dye proved to be troublesome. Frequency doubling was attained by passing the beam through a BBO crystal in a Sirah Second Harmonic Generator.

Jet cooled pure CF_3Br gas was pumped through a 500 μm wide pulsed nozzle from a backing pressure of about 1.5 – 2 bar into a vacuum pumped ionization chamber with a pressure of $5 \cdot 10^{-6}$ mbar. The nozzle was kept open for about 200 μs and the laser pulse was fired 500 μs after the nozzle first opened. The positive ions generated by the laser radiation were extracted into a TOF tube by extractors with a voltage of 1170 V, a repeller with a voltage of 4100 V and the ion beam was focused by two electric lenses with a voltage of 250 V and 3 V. The ions then hit a MCP detector and the signal was fed into a LeCroy WaveSurfer 44MXs-A, 400 MHz storage oscilloscope to measure the signal as a function of time. The average signals were typically recorded for 32 consecutive laser pulses to obtain a mass spectra for a certain excitation energy. Signals were recorded in 0.1, 0.2 and 0.5 cm^{-1} laser wavenumber steps to obtain the 2D-REMPI spectra i.e. mass spectra as a function of laser excitation. 1D-REMPI spectra, i.e. ion signals as a function of laser excitation, for individual ions were obtained by integrating the respective signal areas from the 2D-REMPI spectra for the TOF ranges of the certain ion masses of interest.

Power dependence of the ion signals was determined by averaging the signal over 500 pulses for a certain power. Five quartz windows were used to reduce the original laser power by 59.8 %, 51.1%, 44.6 %, 41.5 % and 34.2 %. Thus for certain laser excitation energies and fixed frequencies the ion signals were measured as a function of varying power.

For all data handling and manipulation the program Igor Pro 4.04 by WaveMatrics was used.

The procedure of this experiment was to scan the excitation region between 71 320 – 84 600 cm^{-1} and gather mass spectra every 0.2 cm^{-1} using REMPI with TOF-MS detection. The scanning region was split up and a total of 142 scans were were made.

.

3 Results & Analysis

The mass spectra obtained by the REMPI measurements proved to be very impure due to a slight spill of vacuum pump motor oil into the ionization chamber. However, this gave an opportunity to use the impurity ion peaks as a standard for calibration of the mass scale. The oscilloscope gives three dimensional data as a function of energy, ion yield and time. This time factor needed to be converted into a mass factor which is relatively easy, given the relationship between the time-of-flight of an ion in the TOF-tube and its mass:

$$t_{TOF} \propto \sqrt{M_w} \tag{3.1}$$

To identify the peaks in the resulting mass spectra, both the impurity mass spectra and CF_3Br mass spectra were collected (Figure 3.1a & 3.1b). The background spectra contained only impurity peaks and the CF_3Br mass spectra contained both signals from the impurity and the CF_3Br molecule. Subtraction of the background spectra from the CF_3Br mass spectra would yield a spectra with peaks that mostly originated from the CF_3Br molecule (Figure 3.1c).

Two peaks in the mass spectra have much larger intensities than others. These peaks can easily be seen in Figures 1a and 1b and are observed due to formation of the C^+ ion from the impurity and N_2^+ which is believed to originate from the atmosphere. These two peaks have known masses and thus the mass axis can be calibrated from - (3.1). In the subtracted spectra it can now be seen that three peaks are more intense than the rest and they have ion masses of 69, 79 and 81 amu and must thus belong to the ions CF_3^+, $^{79}Br^+$ and $^{81}Br^+$ respectively.

In all of the mass spectra only the ions CF_3^+ and Br^+ were observed for CF_3Br. Unlike in the CH_3Br research done by Kvaran et al[2], the mother ion was never observed nor any signal from CF_nBr^+ (n = 0-2), CF_n^+ (n = 1-2), F_2^+, FBr or F^+.

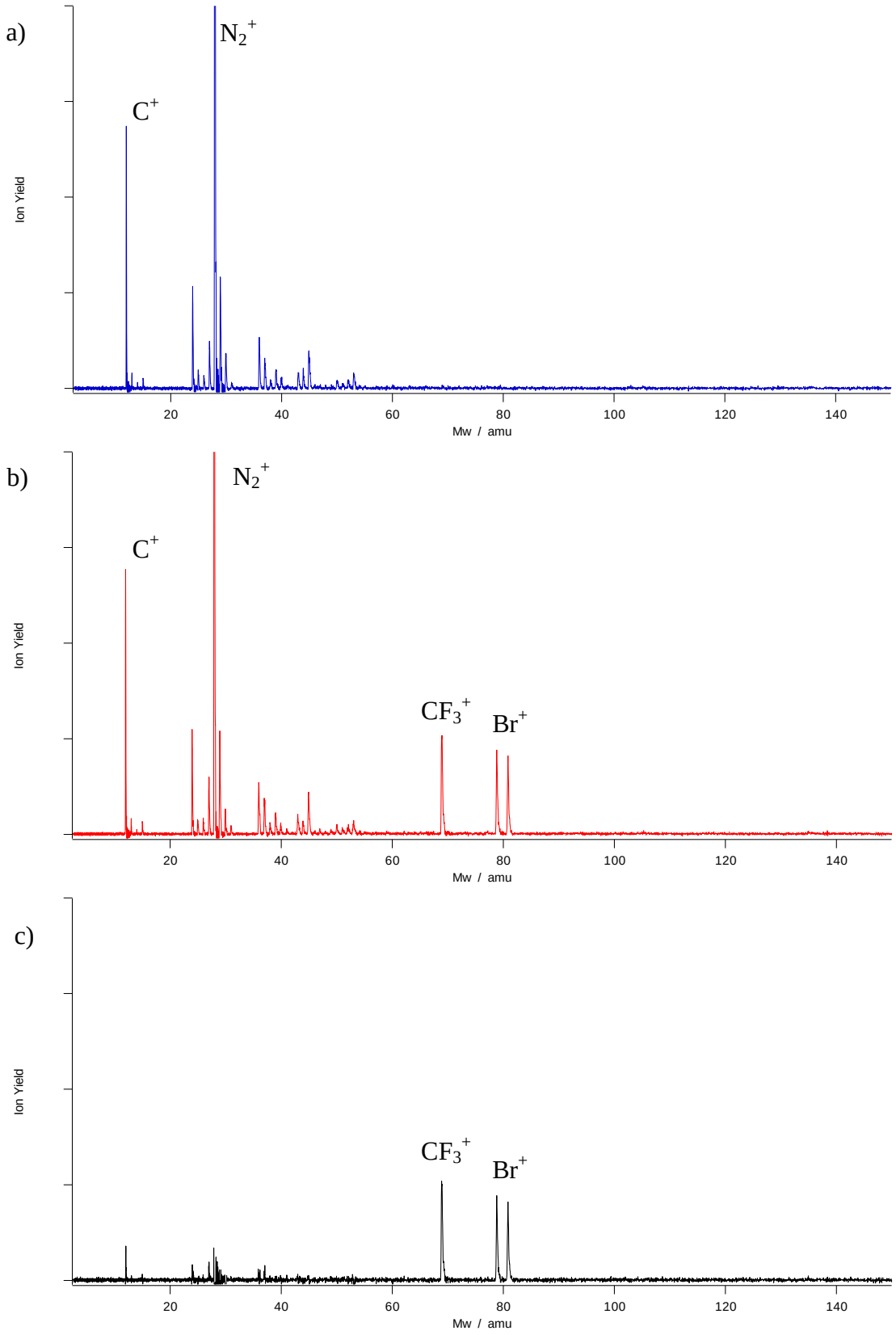

Figure 3.1: a) Impurity mass spectra for the excitation energy 81 800 cm^{-1}. b) Impurity + CF_3Br mass spectra for the excitation energy 81 904 cm^{-1}. c) Subtracted and resulting CF_3Br spectra.

3.1 CF_3^+

Change in intensity of the CF_3^+ ion peak as a function of energy is this chapters main subject and the main results are displayed in the 1D-REMPI spectra in Figure 3.2. In the measured excitation energy region (71 320 – 84 600 cm^{-1}) a CF_3^+ signal was obtained for about 70% of the scanned region, where the signal was observed to be continuous (i.e. not single lines). Due to selection rules of one-photon excitation, allowed transition are $\Delta l = \pm 1$ which explains why the 4p → 5p transition peak is significantly lower than the 4p → 5s for the one-photon spectrum in Figure 3.2. However in this experiment we are observing *(2+n)* photon excitation, meaning that allowed transitions are $\Delta l = 0, \pm 2$, explaining why we mainly observe the 4p → 5p transition. Transitions from 4p → 5s are still possible but the transition probability is so low that no signal is detected meaning that there is insignificant two-photon absorption for these excitation energy regions. It can be seen in the 1D-REMPI spectra of CF_3^+ in Figure 3.2 that a large range from 71 320 – 74 360 cm^{-1} of the plot is missing due to the facts that the transition from 4p → 5s is so unlikely that a signal from CF_3^+ was not observed when this region was measured.

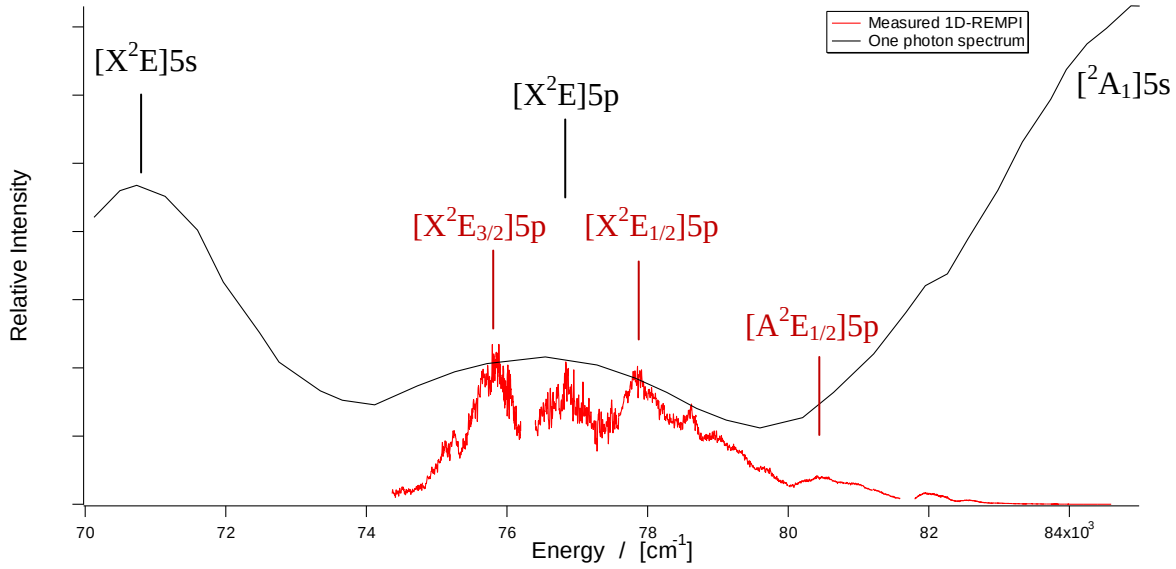

Figure 3.2: 1D-REMPI of CF_3^+ ion signal (red) for the scanned region and the one photon spectral curve (black) along with their respective assignments. An enlarged picture, Figure 4.3, can be found in in the Appendix.

Also it can clearly be noticed that the graph has gaps between 76 200 – 76 400 cm^{-1} and 81 600 – 81 800 cm^{-1} which can be explained with dye laser power. Multiple dyes were required to scan this excitation energy region, as discussed in the experimental setup section, and each of those dyes has a certain laser power curve (see Figure 4.1 and 4.2 in the Appendix for the curves of the dyes used). The position and shape of these laser power curves can be altered by using different concentrations of the dyes. The gaps are formed because of the low laser power obtained at the adjoining points of the dye power curves. This could be fixed by using either another dye or a different concentration of the used dyes, but that was not done in this study due to time restraints.

The graph in Figure 3.2 was constructed in such a way that all 1D-REMPI of CF_3^+ from each scan were gathered into one file. One spectra was chosen to be at a fixed

intensity while the others were then divided by a certain factor in order to fit them together. Where the two gaps appear the signal was assumed to be constant since a dramatic change in the ion yield would have been noted if present. All data was corrected for power, either linearly or by a factor depending on whether the power was changing or constant, according to the relation:

$$I^{corr}(CF_3^+) = \frac{I^{measured}(CF_3^+)}{P^n} \tag{3.2}$$

where I is the signal intensity vector, P is the laser power as a function of dye laser frequency and n is the total number of photons required to yield CF_3^+. n was estimated to be 2 in this case which was confirmed by the power dependent measurements.

For a change in power the power vector required correcting. Each individual scan made, in the measured excitation energy region, is a small portion of the power distribution curves for the dyes seen in Figure 4.1 and 4.2 in the Appendix. Therefore it is safe to assume that the power varies linearly. The correction was therefore done by using a linear interpolation of the power with:

$$P = \left[\frac{(P_e - P_0)}{(\tilde{\nu}_e - \tilde{\nu}_0)}\right] \cdot \tilde{\nu} + \left\{P_0 - \left[\frac{(P_e - P_0)}{(\tilde{\nu}_e - \tilde{\nu}_0)}\right] \cdot \tilde{\nu}_0\right\} \tag{3.3}$$

where P_e is the final power value of the scan, P_o is the inital value, $\tilde{\nu}_e$ is the final wavenumber value, $\tilde{\nu}_0$ is the inital value and $\tilde{\nu}$ is the wavenumber vector for the scan.

No clear sharp CF_3^+ peaks were observed during the scans but after the data manipulation mentioned above a clear pattern in the signal was seen. Comparing it to an absorption spectrum by Eden[5] and Suto and Lee[4] in Figure 3.2 it can be noticed that the total measured 1D-REMPI of CF_3^+ seems to compare to one of the broad peaks in the one-photon spectra which is due to the excitation of CF_3Br to a $[CF_3Br^+ (X^2E)]_c$ 5p Rydberg state. Also, the signal of CF_3^+ vanishes when the energy approaches the $[CF_3Br^+ (^2A_1)]_c$ 5s state absorption region of CF_3Br and it seems to be lowering as well when the energy approaches the $[CF_3Br^+ (X^2E)]_c$ 5s state absorption region. In its ground state CF_3Br has electrons in the 4p orbital of bromine, which are most likely the ones that get excited in the process. This can all be explained with the transition probabilities and selection rules mentioned earlier.

As explained by Clay and Walters *et al*[6], the energy difference between the $X^2E_{3/2}$ and $X^2E_{1/2}$ states is about 2420 cm^{-1} which is close to the spacing between the two peaks shown in Figure 3.2. Possibly the peak at 80 500 cm^{-1} is due to transition to $[CF_3Br^+ (A\ ^2E_{1/2})]_c$ 5p. The peak between those due to the X^2E transitions might be due to an excited vibrational mode of the CF_3Br^{**} molecule.

Formation of a fluorescent CF_3^* fragment can effect the REMPI spectra. As measured by Suto and Lee[4], CF_3^* starts forming and emitting light at about 75 332.15 cm^{-1} and upwards (see Figure 3.4), exactly where the break is noticed in Figure 3.3. Therefore, for this energy there might be competition between direct formation of CF_3^+ and CF_3^* formation. However, power dependent data suggest that the majority of the excited CF_3Br^{**} forms CF_3^+ and as stated by Suto and Lee[4] only 7% of the CF_3Br molecules form

fluorescent CF_3* species. Some portion of the CF_3* might still be ionized to form CF_3^+ by the third photon, but an impact on the 1D-REMPI spectra of CF_3^+ is observed nonetheless.

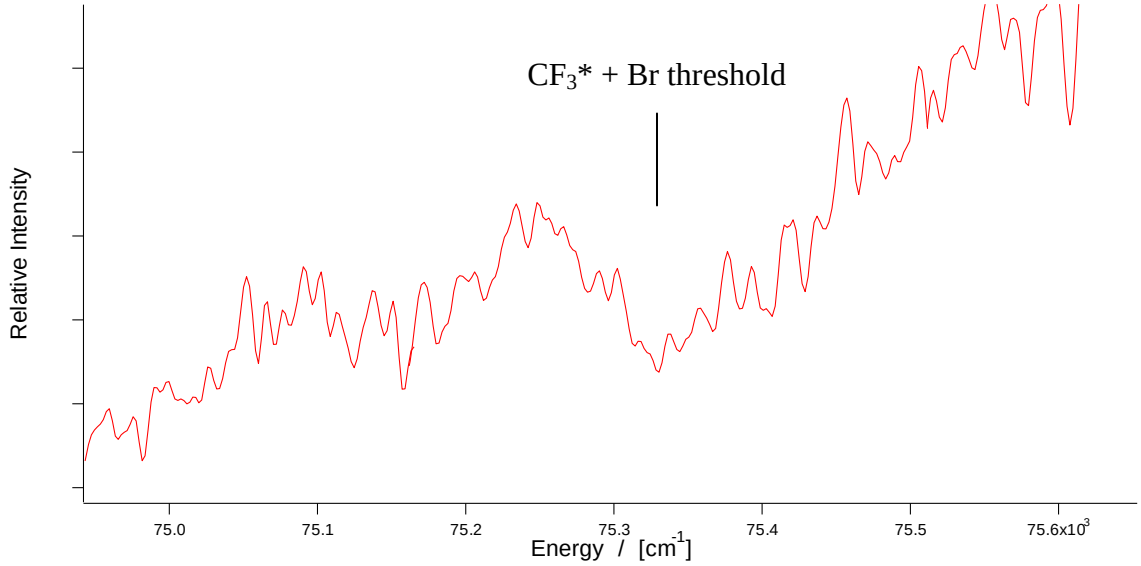

Figure 3.3: Expanded view of the 1D-REMPI for CF_3^+ where the break due to CF_3 formation is to be expected. An enlarged picture, Figure 4.4, can be found in the Appendix.*

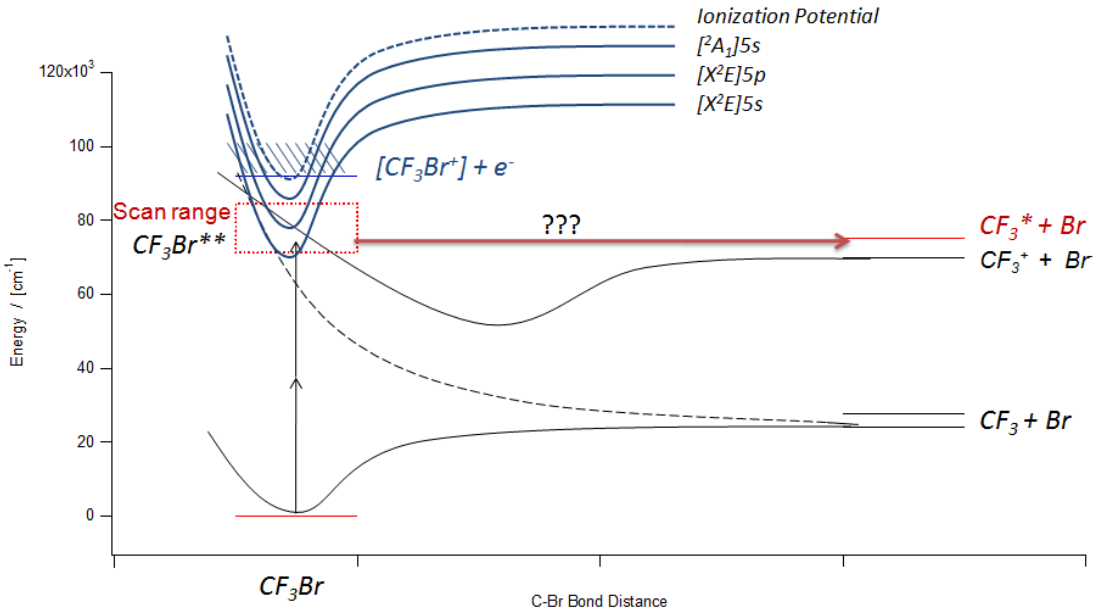

Figure 3.4 : A schematic representation of the suggested dissociation of CF_3Br to form CF_3 and the Rydberg states observed along with the ionization potential curve. The formation mechanism of CF_3* is unknown.*

3.2 Br^+

The bromine ion signal data from the mass spectra was treated in the same way as the CF_3^+ ion signal. There was no continuous bromine ion signal observed in the REMPI spectra but the Br^+ signal appeared as atomic lines, much like those encountered for CH_3Br. A total of 30 bromine atomic lines were observed in the scanned energy region. These are tabulated in Table 3.1 and their position graphed in Figure 3.5 along with the accepted values supplied by NIST[9].

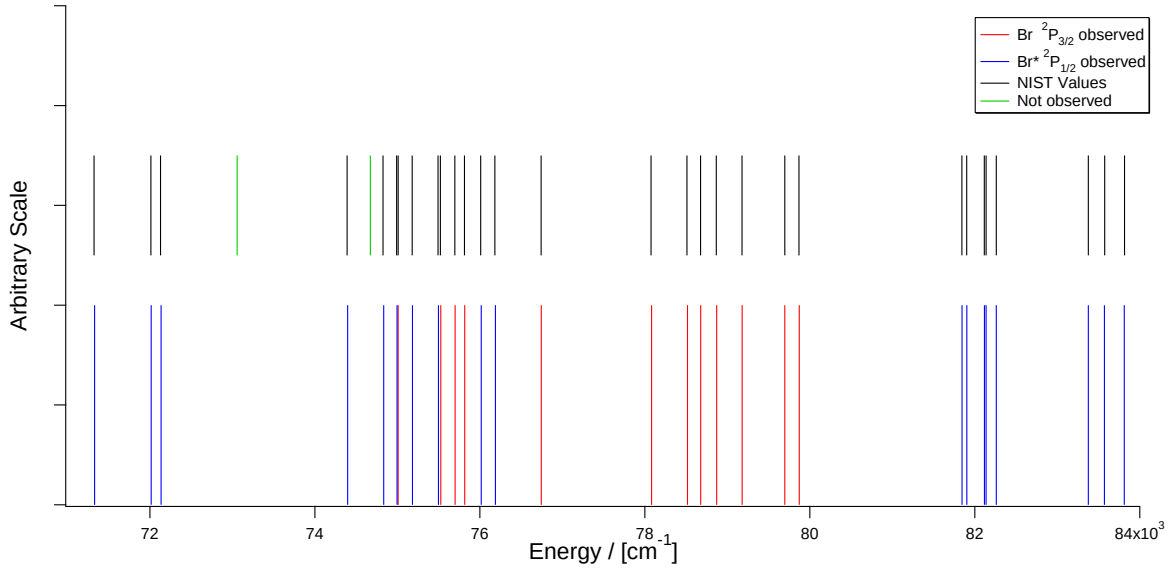

Figure 3.5: Bromine atomic lines (cm^{-1}) due to (2+n) REMPI of $Br(4s^24p^5;^2P_{3/2})$ and $Br^*(4s^24p^5;^2P_{1/2})$ along with theoretical values and the theoretical values that were not observed. An enlarged picture, Figure 4.5, can be found in the Appendix.

As can be seen in Table 3.1 and Figure 3.5 only two allowed transitions were not observed. Three transitions are also not seen because they are unallowed since they don‘t satisfy the selection rule, $\Delta l = 0, \pm 1, \pm 2$.

A problem was encountered when constructing the 1D-REMPI image of Br^+ ion signals. This was due to saturation effects from the bromine signal which resulted in a distorted intensity difference between the saturated peaks and the unsaturated peaks. Also, the power of the laser beam was measured in two different ways and comparison between the peaks measured with different ways proved to be troublesome. Despite these difficulties some bromine lines were compatible with each other. Those lines were corrected accordingly to power and plotted in Figure 3.6 along with the one-photon spectra. They seem to be stronger around the 5p state absorption region but when approaching the 5s Rydberg states absorption region the lines drop immensely in intensity.

[9] (NIST Atomic Spectra Database (Version 4) [2010, November 13])

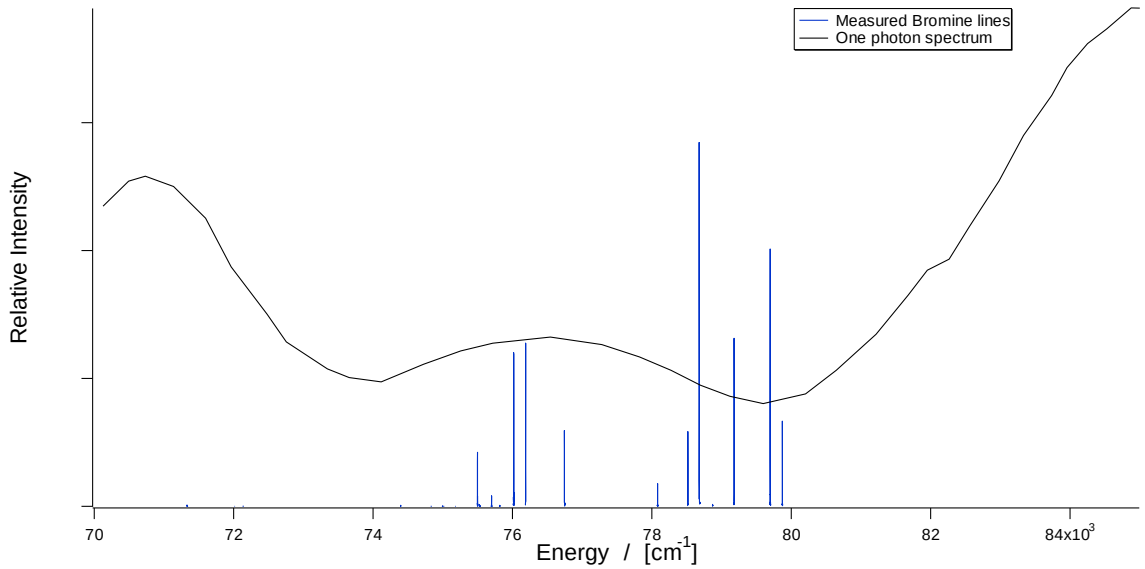

Figure 3.6: 1D-REMPI of usable Br^+ scans (blue) along with the one photon spectrum curve (black). An enlarged picture, Figure 4.6, can be found in the Appendix.

The fact that no continuous bromine signal was observed could suggest that the majority of the CF_3Br dissociation follows the intersystem crossing to an ion-pair state from the $[CF_3Br^+ (X^2E)]_c$ 5p Rydberg state which is a very fast dissociation. However it is much more likely that the excited CF_3Br^{**} molecule enters a repulsive state and forms CF_3 and Br (similar to the CH_3Br research[2,3]). The reason for that is threefold:

- First, it is widely recognized[4,6] that the main photodissociation pathway for CF_3X; X = halogen, is in fact $CF_3X^* \rightarrow CF_3 + X$.
- Second, in the 1D-REMPI of CF_3^+ in Figure 3.2 a break is clearly noticed at 75 332.15 cm^{-1} which is believed to be due to the formation of fluorescent CF_3^* media. It is believed[4] that only about 7% of the excited CF_3Br^* molecules form a fluorescent CF_3^* molecule and the fact that these seven percent have such a huge impact on the 1D-REMPI spectra must mean that the formation of the CF_3^+ observed in the spectra is roughly of the same scale as the CF_3^* formation, say about 10-20%. And since the mother ion was never observed the only possible explanation is that about 75% of the CF_3Br^* molecules dissociate through the repulsive state pathway (1) seen in Figure 3.7.
- Third, the strong Br^+ atomic lines observed which most likely form through a complex mechanism with a total of five photon excitation and involve time delay which shows as saturation in the Br^+ signals point to the fact that the photodissociation $CF_3Br^* \rightarrow CF_3 + Br$ is an important pathway.

A Br^+-continuum is not observed due to the fact that the number of photons required to form a Br^+ signal is too large (five photons in total). Br^+ atomic lines are observed when resonance is present otherwise the signal is not observed because it is to weak. Likewise CF_3^+ ionized from path (1) as seen in Figure 3.7 is probably negligible but CF_3^+ formed via the ion-pair state is strongly observed since only two photons are required for its formation.

The Br^+ formation by path (1) involves time delay which shows as saturation in Br^+ signals. Most likely the excited CF_3Br^{**} loads up in a Rydberg state in the scanned region and then slowly cross over to the repulsive state and dissociate via path (1) while at the same time a small amount of the molecules enter the ion-pair state and follows the fast dissociation via path(3).

Path (2) in Figure 3.7 is thermodynamically possible but the CF_2^+ and F^+ ions were not observed. That might however be due to the same reasons that no continuous Br^+ signal was seen as described above. The energy required to ionize a fluorine atom is 140 524.5 cm^{-1} [9], and using a photon with an average energy of 38 000 cm^{-1} it would require 2+4 photons (or a total of six photons), which is more than what is required to form Br^+ via path (1).

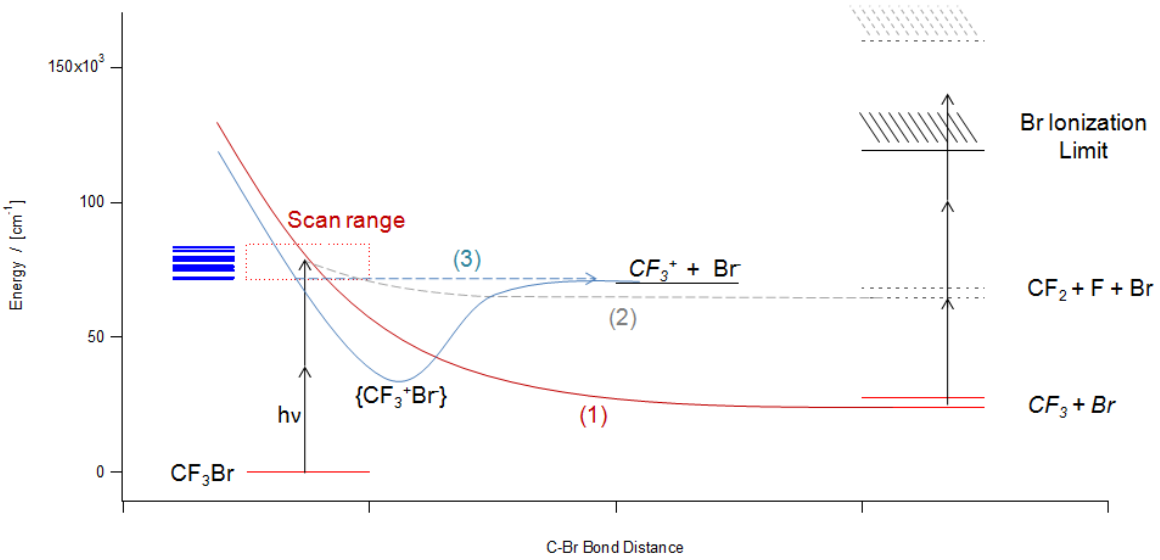

Figure 3.7: Suggested dissociation pathway of CF_3Br. Blue lines represent the bromine energy levels. (1)-Red: Intersystem crossing into a repulsive state to form CF_3 and Br which later ionizes. (2)-Grey: Repulsive state to form CF_2 + F + Br, theoretically possible (but not observed). (3)-Aqua: The direct dissociation of CF_3Br into CF_3^+ and Br^- via Ion-pair state.

Table 3.1 Bromine atomic lines (cm^{-1}) due to (2+n) REMPI of $Br(4s^24p^5;^2P_{3/2})$ and $Br^*(4s^24p^5;^2P_{1/2})$.

		$Br(4s^24p^5;^2P_{3/2})$		**$Br^*(4s^24p^5;^2P_{1/2})$**	
Configuration	terms / $^{2S'+1}X_{J'}$	This work	NIST[9]	This work	NIST[9]
$4s^24p^4(^3P_2)5p$	$^4P_{5/2}$	N/A	74 672.32		
	$^4P_{3/2}$	75 010.0	75 009.13	71 330.4	71 323.89
	$^4P_{1/2}$	75 817.6	75 814.00	72 135.6	72 128.76
	$^4D_{7/2}$	75 526.8	75 521.50	Unallowed	
	$^4D_{5/2}$	75 700.4	75 697.05	72 015.2	72 011.81
	$^4D_{3/2}$	76 745.2	76 743.08	N/A	73 057.84
$4s^24p^4(^3P_1)5p$	$^2S_{1/2}$	78 082.4	78 076.00	74 396.8	74 390.76
	$^2D_{5/2}$	78 516.8	78 511.60	74 834.0	74 826.36
	$^2D_{3/2}$	78 678.4	78 676.65	74 995.6	74 991.41
	$^4D_{1/2}$	78 870.8	78 865.72	75 184.0	75 180.48
	$^4S_{3/2}$	79 179.6	79 178.33	75 498.0	75 493.09
$4s^24p^4(^3P_0)5p$	$^2P_{3/2}$	79 696.8	79 695.89	76 016.4	76 010.65
	$^2P_{1/2}$	79 872.0	79 868.03	76 189.2	76 182.79
$4s^24p^4(^3P_2)6p$	$^4P_{5/2}$			81 844.8	81 842.58
	$^4P_{3/2}$			81 903.3	81 902.06
	$^4P_{1/2}$			82 116.9	82 114.95
	$^4D_{7/2}$			Unallowed	
	$^4D_{5/2}$			82 136.9	82 136.29
	$^4D_{3/2}$			82 260.9	82 259.62
$4s^24p^4(^1D)5p$	$^2F_{5/2}$			83 376.0	83 376.99
	$^2F_{7/2}$			Unallowed	
	$^2P_{3/2}$			83 572.0	83 575.05
	$^2P_{1/2}$			83 812.0	83 814.79

3.2.1 CF_3Br vs CH_3Br

In Figure 3.8 the comparison between the bromine lines for CH_3Br and CF_3Br can be seen. The main difference between the two is that for CH_3Br the measurements yielded a continuous Br^+ signal where as in CF_3Br it did not.

Furthermore, there is no obvious relationship between the bromine lines observed for CH_3Br by Kvaran *et al*[2] and the lines observed for CF_3Br and there is a significant difference in their relative intensities. The very strong bromine line observed for CH_3Br ($^4D_{3/2} \leftarrow\leftarrow {}^2P_{3/2}$) at 76 743 cm^{-1} is only of medium intensity for CF_3Br and the second most intense lines for CH_3Br ($^4D_{7/2} \leftarrow\leftarrow {}^2P_{3/2}$ and $^2S_{1/2} \leftarrow\leftarrow {}^2P_{3/2}$) are weak for CF_3Br.

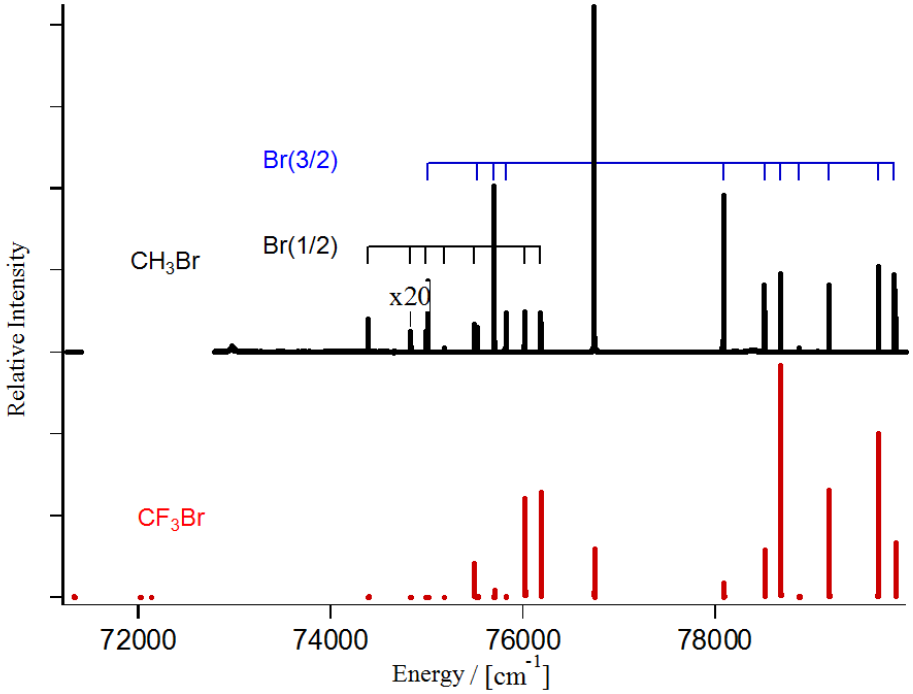

Figure 3.8: Comparison between bromine atomic lines from CH_3Br (black) and CF_3Br (red).

3.3 C^+

The presence of carbon atomic lines was not observed until near the end of the experiment. Up to that point the C^+ signal was always assumed to originate from the vacuum pump-oil impurity and were therefore ignored. The thermodynamics of the bond-breaking of CF_3Br do not support the formation of C^+ with the corresponding energy assuming *(2+n)* REMPI, yet clearly carbon atomic lines from CF_3Br are observed. This was tested by measuring both the impurity and the sample with the same parameters and the intensities of the atomic lines compared.

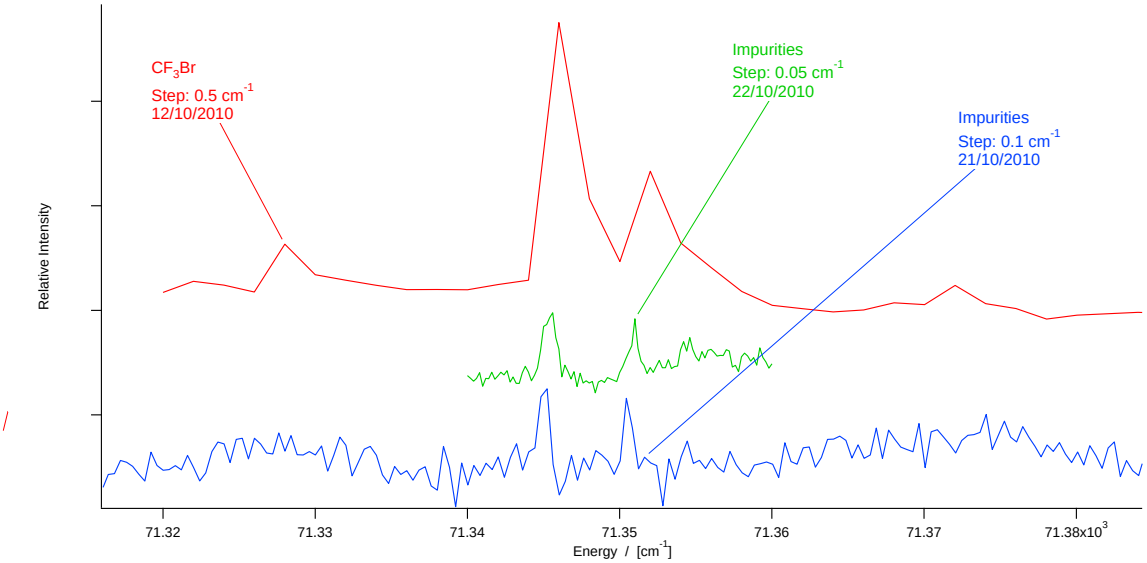

Figure 3.9: The strongest carbon atomic lines observed for both CF_3Br and the impurities present. Intensities have been corrected in terms of power with the estimated value of n=2 for equation (3.2).

The intensity difference between the carbon atomic line peaks can not be explained with only relations to variable laser power output. It can not be explained through thermodynamics since the lowest energy required to form a carbon atom from CF_3Br is 117 783 cm^{-1} [7,10,11] and the highest photon energy used in this experiment was 84 600 cm^{-1} (combined energy of two photons). As can be seen in Figure 3.10 the energy level for the formation of a carbon atom is much greater than the scanned energy region following two-photon resonance excitation. More importantly in order to yield a C^+ ion it would require about 208 603 cm^{-1} of energy[9] making the formation of C^+ peaks even more thermodynamically unfavorable.

[10] (CRC Handbook of chemistry and physics, 63rd edition, 1982-1983)
[11] (Comprehensive handbook of chemical bond energies, 2007)

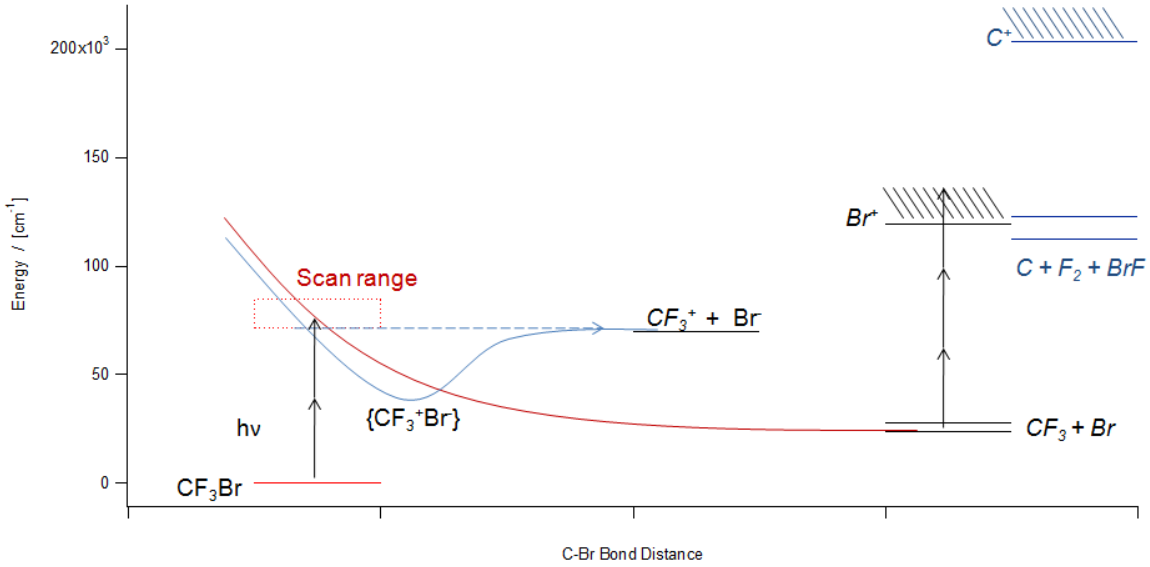

Figure 3.10: The suggested dissociation pathway of CF_3Br along with the thermodynamical energy levels for the formation of a carbon atom and a C^+ ion.

Many carbon lines were not observed due to long scan steps used for the region of concern and lack of laser power. Smaller steps and more laser power might reveal more carbon atomic lines. The observed carbon atomic lines were tabulated and their positioned graphed just like the bromine atomic lines. The results can be found in Table 3.2 and Figure 3.11.

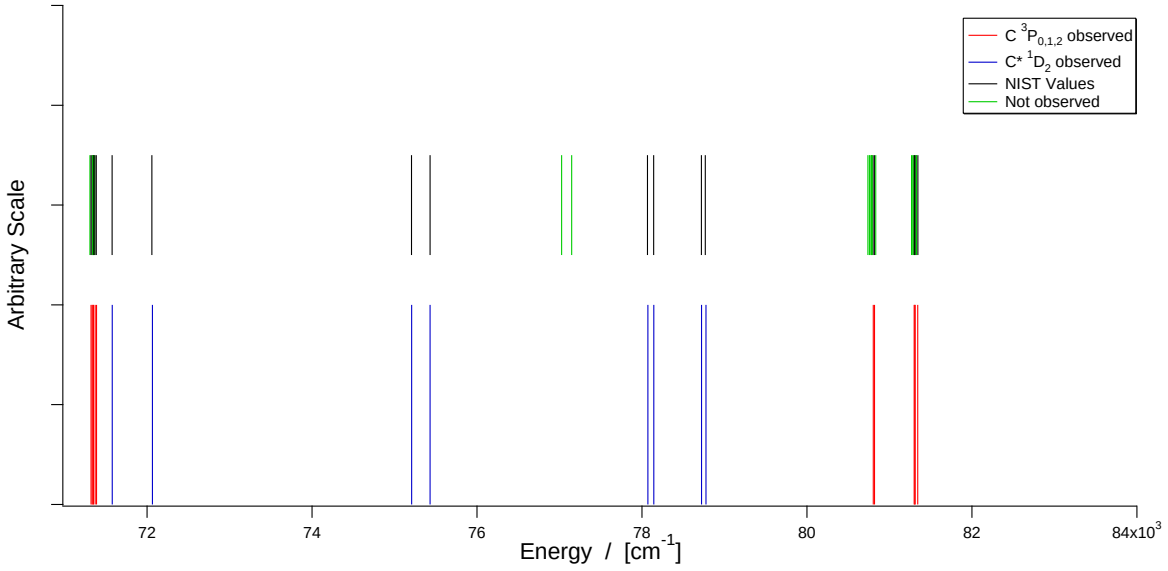

Figure 3.11: Carbon atomic lines (cm^{-1}) due to (2+n) REMPI of $C(2s^22p^2;^3P_{0,1,2})$ and $C^*(2s^22p^2;^1D_2)$ along with theoretical values the theoretical values that were not observed. An enlarged picture, Figure 4.7, can be found in the Appendix.

A large error can be noticed between the position of this works carbon atomic lines and the theoretical values supplied by NIST[9], this is mainly because of the long scan steps and the lack of laser power making the signal weak and the position of the peak therefore more ill defined. The strongest carbon lines were due to the transitions $2s^2 2p3p;^3P_0 \leftarrow\leftarrow 2s^2 2p^2;\ ^3P_0$ at 71 352 cm^{-1} and $s^2 2p3p;^3P_1 \leftarrow\leftarrow 2s^2 2p^2;\ ^3P_1$ at 71 346 cm^{-1} for the two ground state excitations of the carbon. For the excited carbon atomic lines the $^1D_2$ lines were always stronger than the $^1S_0$ lines in intensity by about one third which very much resembles the CH_3Br research[2].

No complete 1D-REMPI for the C^+ ion signal was constructed because the signal was weak and the scans were not internally compatible, meaning that despite linear laser power corrections there seemed to be no relationship between the intensity of the peaks just like for the Br^+ ion signal. In this case it was due to difficulties in linear correction of the signal with relations to power which stemmed from the fact that the number of photons required to form a C^+ ion (see the *n* factor of equation 3.2) is unknown for CF_3Br.

Table 3.2: Carbon atomic lines (cm^{-1}) due to (2+n) REMPI of $C(2s^2 2p^2;^3P_{0,1,2})$ and $C^*(2s^2 2p^2;^1D_2)$.

		$C(2s^2 2p^2;^3P_0)$		**$C(2s^2 2p^2;^3P_1)$**		**$C(2s^2 2p^2;^3P_2)$**	
Configuration	terms / $^{2S'+1}X_{J'}$	This work	NIST[9]	This work	NIST[9]	This work	NIST[9]
$2s^2 2p3p$	$^3P^0$	71 352.01	71 351.51	71 336.00	71 335.11		
	$^3P^1$		71 364.90	71 346.01	71 348.50	71 322.01	71 321.50
	$^3P^2$	71 388.06	71 385.38	71 372.05	71 368.98		71 341.98
$2s^2 2p4p$	$^3D^1$		80 782.51		80 766.11		80 739.11
	$^3D^2$	80 804.00	80 801.27		80 784.87		80 757.87
	$^3D^3$		80 834.61	80 820.00	80 818.21		80 791.21
	$^3P^0$	81 310.15	81 311.01		81 294.61		81 267.61
	$^3P^1$		81 325.67	81 310.15	81 309.27		81 282.27
	$^3P^2$	81 342.24	81 343.99		81 327.59	81 300.12	81 300.59

		$C^*(2s^2 2p^2;^1D_2)$	
Configuration	terms / $^{2S'+1}X_{J'}$	This work	NIST[9]
$2s^2 2p4p$	$^1D_2$	71 578.93	71 577.16
	$^1S_0$	72 065.55	72 059.08
$2s^2 2p5p$	$^1D_2$	75 208.01	75 207.18
	$^1S_0$	75 431.00	75 432.55
$2s^2 2p6p$	$^1D_2$		77 025.63
	$^1S_0$		77 148.41
$2s^2 2p7p$	$^1D_2$	78 072.06	78 067.74
	$^1S_0$	78 144.26	78 141.35
$2s^2 2p8p$	$^1D_2$	78 723.32	78 720.93
	$^1S_0$	78 755.78	78 768.01
$2s^2 2p9p$	$^1D_2$		79 157.47
	$^1S_0$		79 188.98
$2s^2 2p10p$	$^1S_0$		79 485.48

3.4 Power Dependence

Measurements of power dependence were done for the CF_3^+ and Br^+ ion peak signals. The data for the latter proved to be unusable due to saturation effects and will therefore have to be repeated.

For each power dependence scan the data was handled with care. The respective peaks were carefully integrated and the power of each peak recorded. A graph was then made by plotting up the logarithm of both the peak area and the power. Linear curve fitting gave a slope value which revealed the number of photons needed to create the respective ion. Few lines with integer slopes were also added to the graph for clarity. The resulting graphs looked typically like Figure 3.12 and the rest of the power dependence data can be found in the Appendix in Chapter 4.3. The measurements for CF_3^+ power dependence and their data are tabulated in Table 3.3.

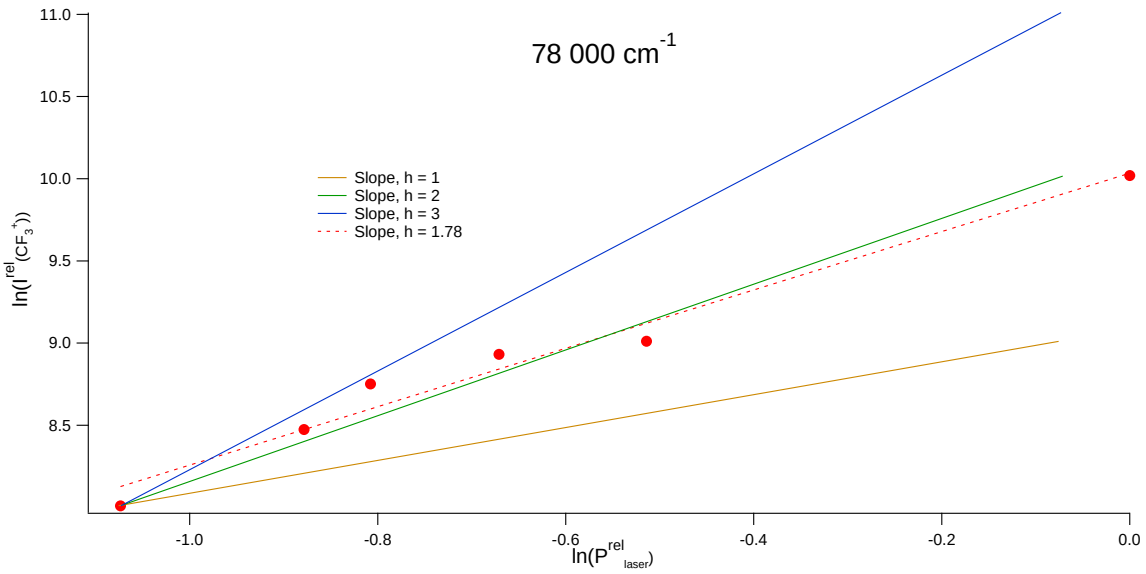

Figure 3.12: Resulting graph from a single power dependence scan for the excitation energy 78 000 cm^{-1} with data in form of points, the linear curve fit (red dashed) and three lines with integer slopes.

Table 3.3: CF_3^+ power dependence measurements. The position in energy, the linear curve fit slope and the evaluated integer slope for each scan revealing the number of photons required to ionize CF_3.

Energy / [cm^{-1}]	α	$\alpha_{eval.}$
77200	2.18 ± 0.51	2
77600	1.77 ± 0.30	2
78000	1.78 ± 0.14	2
78400	1.46 ± 0.22	2†
78800	1.63 ± 0.12	2
79200	1.69 ± 0.15	2
79600	1.75 ± 0.10	2
80000	2.16 ± 0.08	2
80400	1.81 ± 0.06	2
80800	2.11 ± 0.06	2
81200	2.14 ± 0.10*	2
81600	2.25 ± 0.22*	2

*: the average value of two scans for the same energy. †: the low power data supply a slope closer to 2.

It can clearly be seen that for this energy region two photons are required to form the CF_3^+ species, suggesting that the signal observed mainly originates form the ion-pair dissociation path (3) in Figure 3.7. This justifies the corrections made for the CF_3^+ signals with respect to variable laser power. This does not support the repulsive state dissociation pathway, since it would require four photons to yield a CF_3^+ cation in that way, however the power dependence results do not exclude the theory that most of the CF_3^+ is formed via that path. The fact that the CF_3^+ signal from path (1) in Figure 3.7 is so weak means that the power dependence scans only record the CF_3^+ formed with path (3) and it can therefore be stated that the CF_3^+ ions observed are mostly being formed by ion-pair dissociation.

4 Conclusions

CF_3Br was analyzed with *(2+n)* REMPI-TOF for the resonance excitation energy region 71 320 – 84 600 cm^{-1}. The ion peaks of the mass spectra were further analyzed to yield 1D-REMPI. Only CF_3^+, Br^+ and C^+ signals were observed.

The CF_3^+ signal was continuous and slightly changing as seen in Figure 3.2, the Br^+ signal and C^+ signal consisted only of atomic lines and these lines were compared to theoretical values supplied by NIST[9] (Table 3.1 and 3.2). This led to the conclusion that the dissociation of CF_3Br over this laser energy interval follows the pathway of an ion pair dissociation after first having been excited to a $[CF_3Br^+ (X^2E)]_c$ 5p Rydberg state and a pathway of repulsive state dissociation to form CF_3 and Br radicals which later were ionized. Bromine atomic lines are formed when the molecule intersystem crossed from a Rydberg state to a repulsive state and the photon energy was in resonance with a bromine atomic level. The main dissociation pathway is most likely the repulsive state dissociation via path (1) in Figure 3.7 (see discussion and list in Chapter 3.2). CF_3^+ signal from path (1) was not observed because too many photons were required to ionize the CF_3 radical.

Another possible dissociation pathway is path (2) in Figure 3.7, the repulsive state dissociation to form CF_2, F and Br radicals. It is theoretically possible but was not observed in this research due to the number of photons required to ionize the radicals formed in this dissociation path. Path (2) is less likely to occur than path (1) since it's thermodynamically higher in energy.

Ion-pair dissociation via path (3) was the only pathway observed. However, it is believed that only a small fraction of the CF_3Br molecules dissociate via ion-pair dissociation.

With the results from this study it is not really possible to tell which dissociation path is the major pathway and what ratio of excited CF_3Br^* molecules dissociate via each path with full certainty. However, path (1) is the most likely dissociation path as mentioned in Chapter 3.2. Paths (2) and (3) are less likely but present as well as the formation of a fluorescent CF_3^* species. The effect of excited fluorescent CF_3^* species was observed in the CF_3^+ 1D-REMPI spectrum but the effect and formation of the species is believed to be minimal as compared to CF_3^+. The carbon atomic lines remain unexplained, since the formation of a carbon atom is not thermodynamically favorable for this energy region following two-photon resonance excitation.

Power dependence measurements were done on the CF_3^+ and Br^+ signals. The results were that two photons are required to form the CF_3^+ species observed in these scans and therefore the cation stems from the ion-pair dissociation path. It did not exclude the theory that CF_3^+ is mainly being formed by the repulsive state described in Figure 3.7. Inconsistency in the Br^+ power dependence measurements led to no results thereof, most likely due to saturation effects from the bromine signal, and therefore the measurements need to be redone.

References

(1) *Environmental Chemistry - 4th edition*. **Baird, C.; Cann, M. 2008**. 2008, W.H. Freeman and Company.

(2) *Two-Dimensional (2+n) REMPI of CH_3Br: Photodissociation Channels via Rydberg States*. **Kvaran, Á.; Wang, H.; Matthíasson, K. 2010**. 2010, Journal of Physical Chemistry, Vol. 114, No. 37, P. 9991.

(3) *Vacuum ultraviolet absorption spectra of the bromomethanes*. **Causley, G.C.; Russel, B.R. 1975.** 1975, Journal of Chemical Physics, Vol. 62, No. 3, P. 848.

(4) *Emission spectra of CF_3 radicals. V. Photodissociation of CF_3H, CF_3Cl, and CF_3Br by vacuum ultraviolet.* **Suto, M.; Lee, L.C. 1983**. 1983, Journal of Chemical Physics, Vol. 79, No. 3, P. 1127.

(5) *VUV photoabsorption in CF_3X (X = Cl, Br, I) fluoro-alkanes.* **Eden, S.; Limão-Vieira, P.; Hoffmann, S.V.; Mason, N.J. 2005.** 2006, Chemical Physics, Vol. 323, P. 313.

(6) *Photoionization of gas-phase bromotrifluoromethane and its complexes with methanol: State dependence of intracluster reactions.* **Clay, J.T.; Walters, E.A.; Grover, J.R.; Willcox, M.V. 1994**. 1994, Journal of Chemical Physics, Vol. 101, No. 3, P. 2069.

(7) *Handbook of bond dissociation energies in organic compounds*. **Yu-Ran Luo**. 2003, CRC Press.

(8) *Electron impact excitation and dissociation of halogen-containing molecules.* **Kitajima, M; Suzuki, R; Tanaka, H; Pichl, L; Cho, H. 2003**. 2003, Nukleonika, Vol. 48, No. 2, P. 89.

(9) *NIST Atomic Spectra Database (Version 4) [2010, November 13]*, [Online]. Available: http://www.nist.gov/pml/data/asd.cfm. National Institute of Standards and Technology, Gaithersburg, MD.

(10) *CRC Handbook of chemistry and physics, 63rd edition, 1982-1983.* **Weast, R.C.**

(11) *Comprehensive handbook of chemical bond energies.* **Yu-Ran Luo**. 2007, CRC Press.

Appendix

4.1 Dye laser power curves

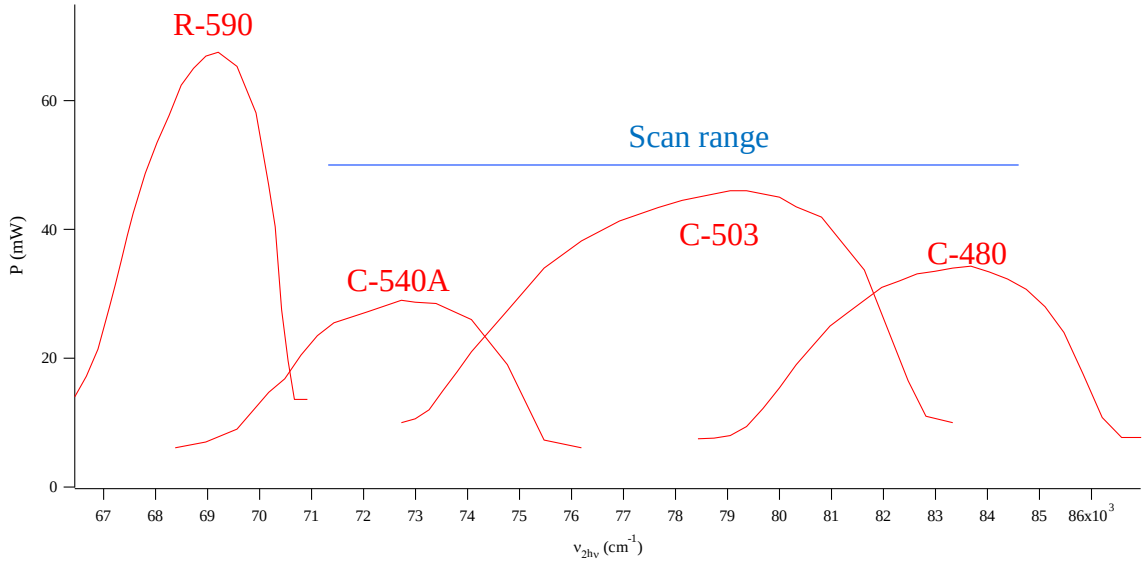

Figure 4.1: Power curves for dyes C-480, C-503, C-540A and R-590 (Red) along with a blue line depicting the scan range of this research. The height, position and form of the curves might be a little distorted due to different concentrations of the dyes used during the measurements.

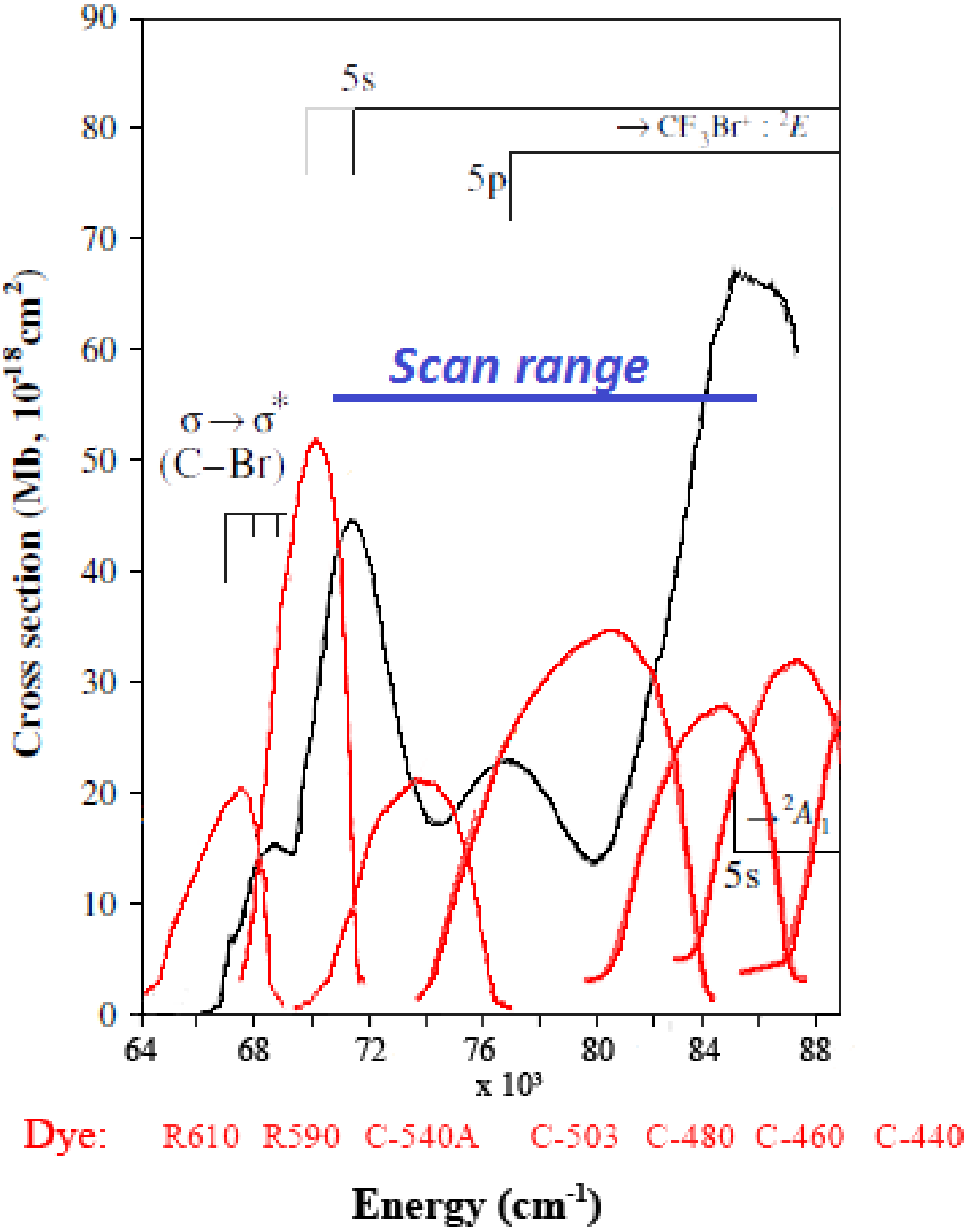

Figure 4.2: Power curves for the respective dyes (RED) appended to the one-photon absorption spectra of CF3Br provided by Eden et al[5], along with a blue line depicting the scan range of this research. The height, position and form of the curves might be a little distorted due to different concentrations of the dyes used during the measurements.

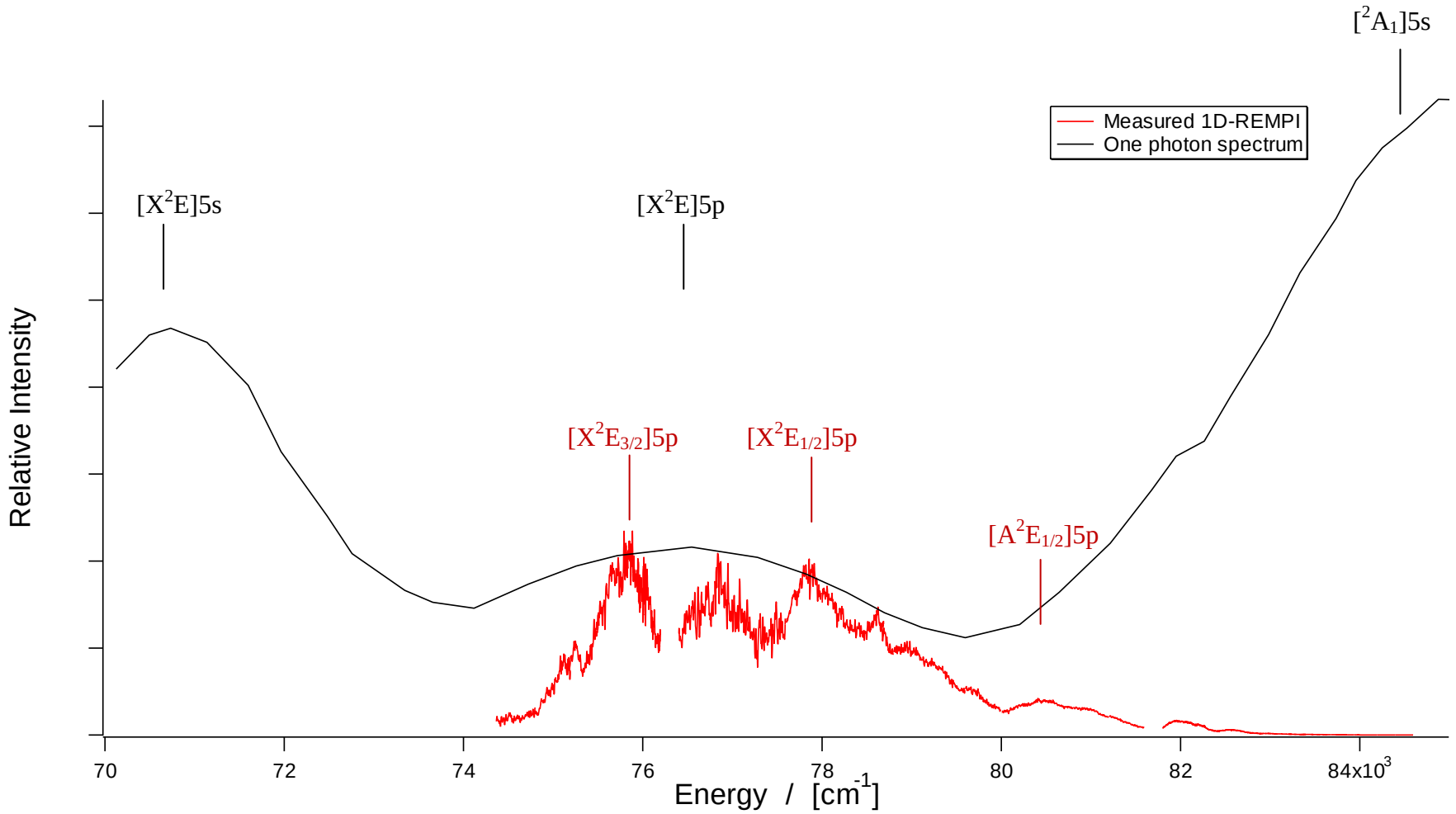

Figure 4.3: Enlarged 1D-REMPI of CF_3^+ ion signal (red) for the scanned region and the one photon spectral curve (black) along with their respective assignments.

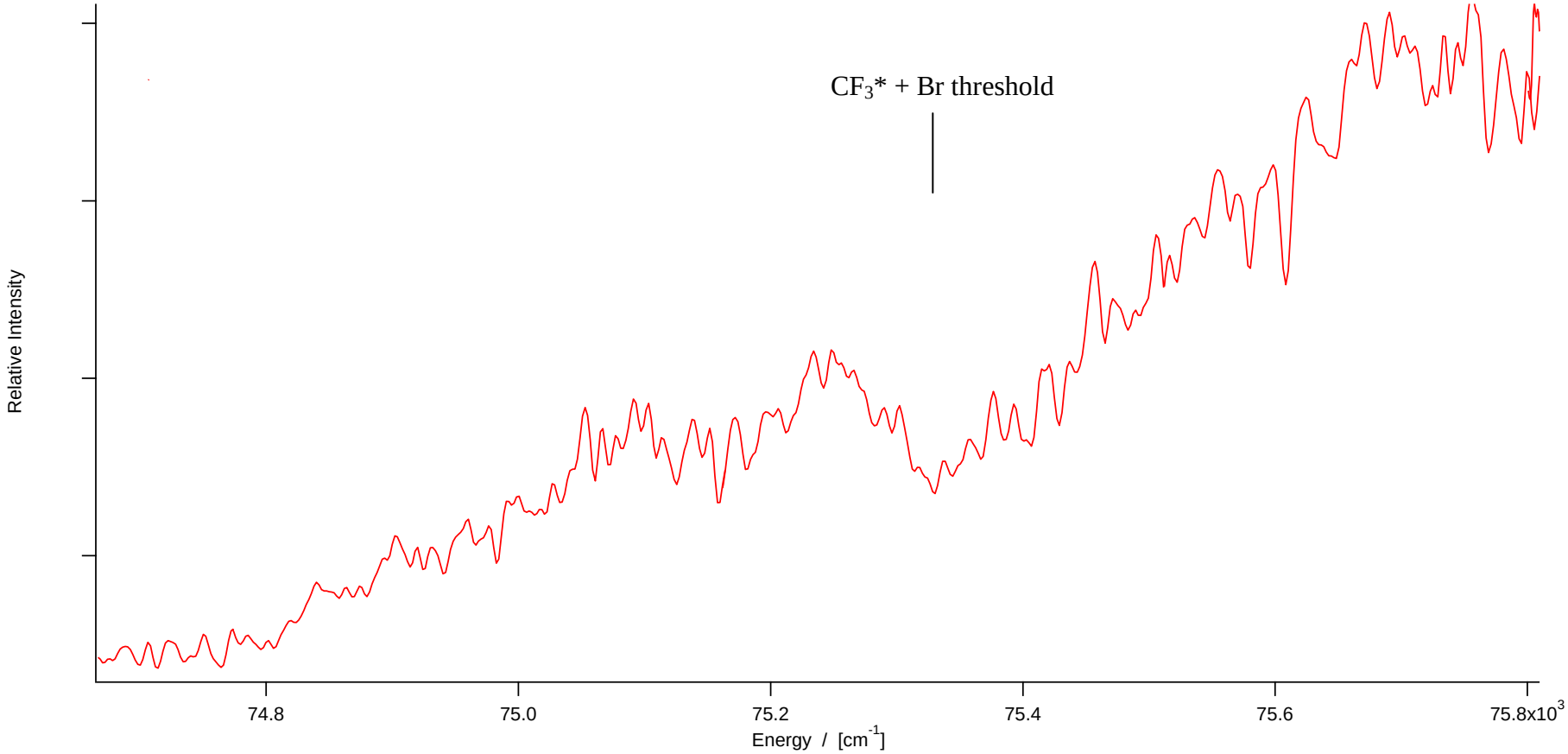

Figure 4.4: Enlarged and expanded view of the 1D-REMPI for CF_3^+ where the break due to CF_3 formation is to be expected.*

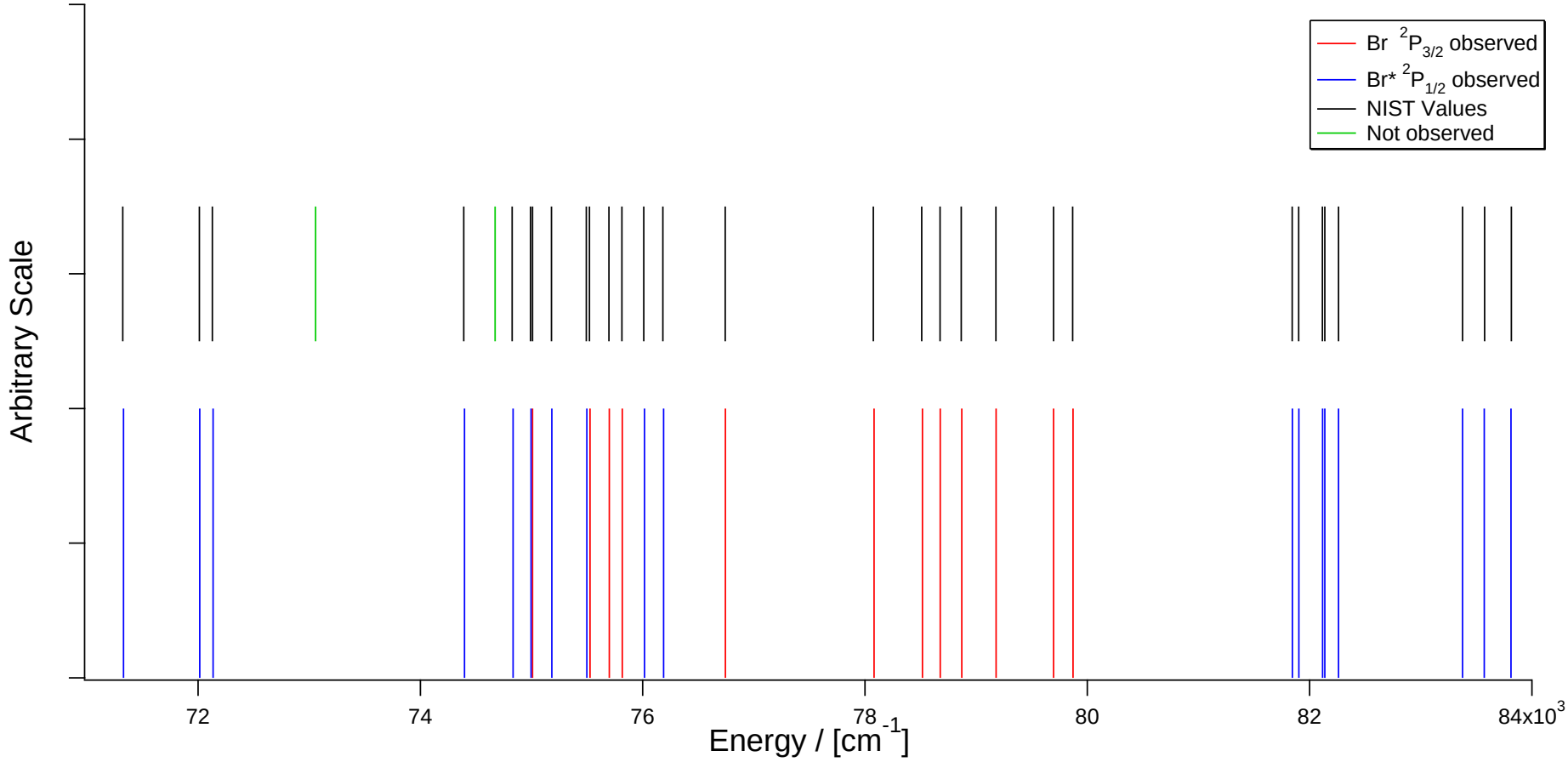

Figure 4.5: Enlarged bromine atomic lines (cm^{-1}) due to (2+n)-REMPI of Br($4s^24p^5;^2P_{3/2}$) and Br($4s^24p^5;^2P_{1/2}$) along with theoretical values and the theoretical values that were not observed.*

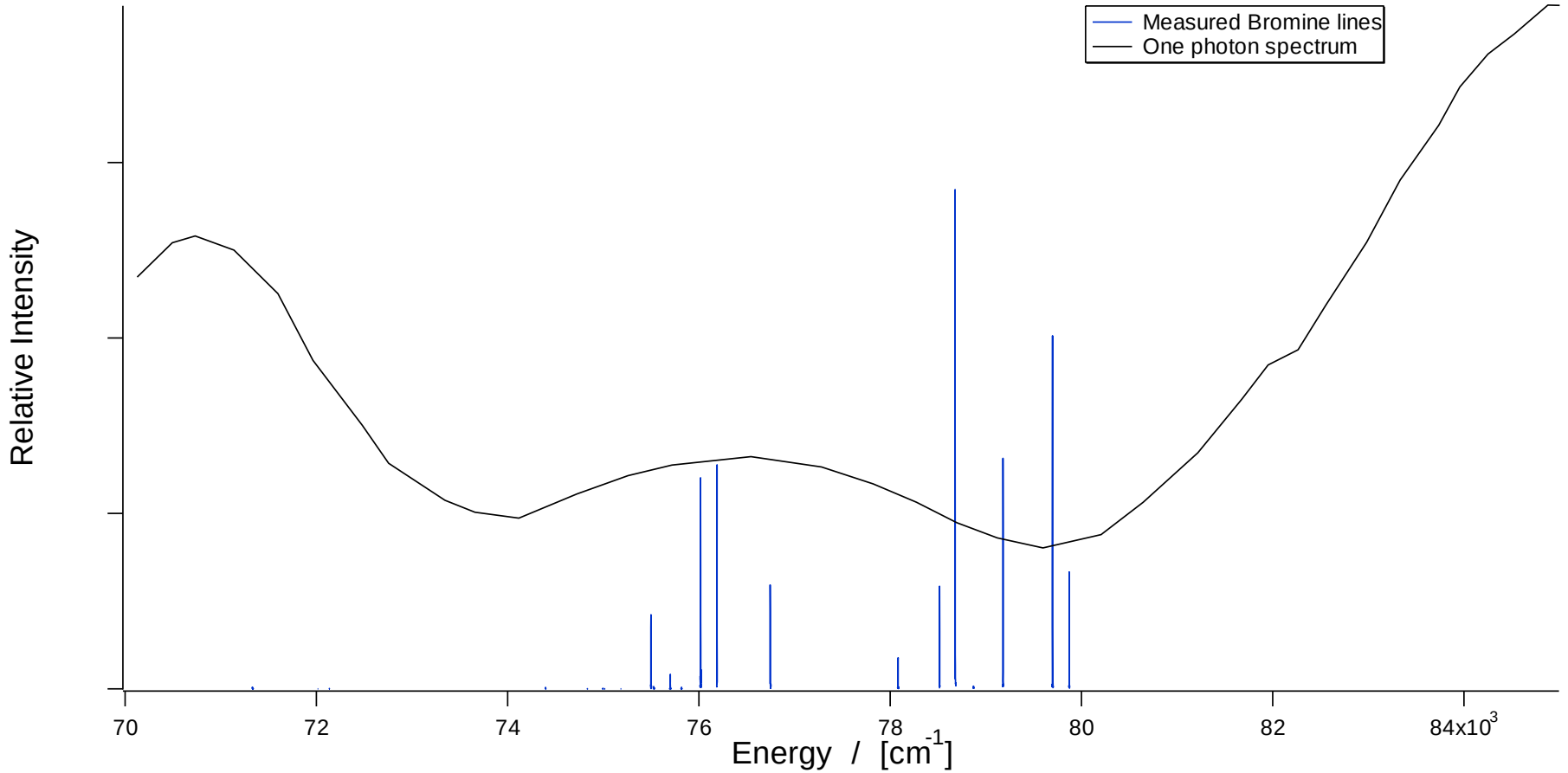

Figure 4.6: Enlarged 1D-REMPI of usable Br^+ scans (blue) along with the one photon spectrum curve (black).

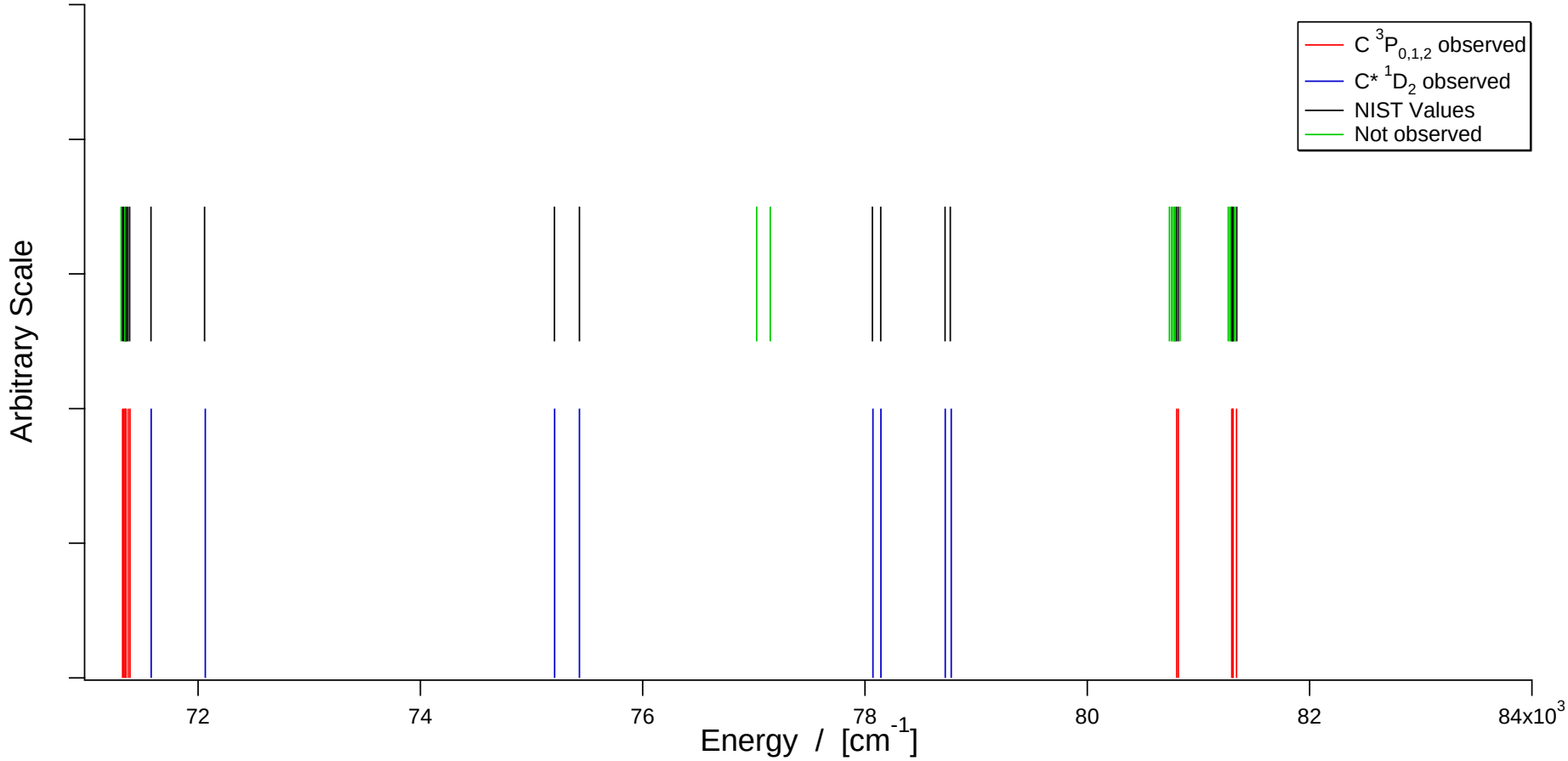

Figure 4.7: Enlarged carbon atomic lines (cm^{-1}) due to (2+n)-REMPI of $C(2s^22p^2;^3P_{0,1,2})$ and $C^*(2s^22p^2;^1D_2)$ along with theoretical values the theoretical values that were not observed.

4.2 Igor code

4.2.1 Mass axis calibration

```
#pragma rtGlobals=1                    // Use modern global access method.
macro UsecursorA()
showinfo
variable tureorfalse
tureorfalse=exists("massreference")
if (tureorfalse==1)
killwaves massreference
killwaves masspoint
make/n=0 massreference
make/n=0 masspoint
else
make/n=0 massreference
make/n=0 masspoint
endif
endmacro
macro Addreference(mass)
variable mass
prompt mass,"Please input its mass:"
variable x1
x1=hcsr(A)
insertpoints 0,1,massreference
insertpoints 0,1,masspoint
massreference[0]=mass
masspoint[0]=x1
endmacro
macro Producemasssaxis(masspoints)
variable masspoints
prompt masspoints,"Please input the number of mass spectra points"
variable tureorfalse
tureorfalse=exists("constants")
if (tureorfalse==1)
killwaves constants
make/d/n=2 constants={0,0}
else
make/d/n=2 constants={0,0}
endif
funcfit /h="00" massfit constants masspoint /x=massreference /d
display masspoint vs massreference
modifygraph mode(masspoint)=3, rgb=(0,0,0)
appendtograph fit_masspoint
tureorfalse=exists("massaxis")
if (tureorfalse==1)
else
make/n=(masspoints) massaxis
endif
massaxis=((x-constants[1])/constants[0])^2

variable i=0
if(constants[1]>0)
do
massaxis[i]=-massaxis[i]
i+=1
while(i<constants[1])
endif
```

```
doalert 0, "Ok! You get a mass axis. Its name is 'massaxis' ! Now you can change x with new axis :)"
killwaves constants
killwaves W_ParamConfidenceInterval
killwaves W_sigma
endmacro
function massfit(constants, m):FitFunc
wave constants
variable  m
return  constants[0]*m^0.5+constants[1]
end
```

4.2.2 REMPI Integration

```
#pragma rtGlobals=1                    // Use modern global access method.
menu "Macros"
"Set Integrate area"
"REMPIIntegrate"
end
macro REMPIIntegrate(wavestart,waveend,finallyname)
string wavestart
string waveend
variable startpoint
variable endpoint
string finallyname
prompt wavestart,"Beginning Wavename: "
prompt waveend,"Ending Wavename: "
prompt finallyname,"Beginning Wavename: "
variable/G wavenum              //getthe number in  input  wavename  and global
string wavenameconstant      //set "wave" as a string constant
wavenameconstant="wave"
variable startwave
variable endwave
variable wavedeta
variable eachwaveintegrate
string wavenam
variable x1
variable x2
variable detax
x1=pcsr(A)
x2=pcsr(B)
if (x1<x2)
startpoint=x1
endpoint=x2
else
startpoint=x2
endpoint=x1
endif
detax=endpoint-startpoint
getwavenum(wavestart)           //use "getwavenum" function to get the number
startwave=wavenum
getwavenum(waveend)
```

```
endwave=wavenum
wavedeta=endwave-startwave+1   //obatin the delta between start wave and end wave
make/N=(wavedeta) $finallyname    //make a new wave, and name as user defined
variable i
i=0
variable yaveragevalue
do
wavenam=wavenameconstant+num2str(i+startwave)
if (mean($wavenam,startpoint-2,startpoint+2)<mean($wavenam,endpoint-2,endpoint+2))
yaveragevalue=mean($wavenam,startpoint-2,startpoint+2)
else
yaveragevalue=mean($wavenam,endpoint-2,endpoint+2)
endif
$finallyname[i]=area($wavenam,startpoint,endpoint)-detax*yaveragevalue
i+=1
while(i<wavedeta)
print " O k !   You get the wave name is: "+finallyname
display $finallyname
killvariables/A
endmacro
macro SetIntegratearea()
showinfo
endmacro
function getwavenum(wavenam)       //this function is used to find the number of wave
string wavenam
variable/G wavenum
sscanf wavenam,"wave%f", wavenum
end
```

4.2.3 Power Dependence Integration

```
include <AreaXY> menus=0
Menu "Macros"
        "Integral berechnen",  Integralberechnung()
End
Macro PutCursorsOnWave(w)
        String w
        Prompt w,"wave to put cursors on",popup,TraceNameList("",";",1)
        ShowInfo;Cursor/P A,$w,0;Cursor/P B,$w,numpnts(TraceNameToWaveRef("",w))-1
End
Function fAreaXYBetweenCursors()
        String wvaName,wvbName,wvxName
        WAVE wva=CsrWaveRef(A)
        WAVE wvb=CsrWaveRef(B)
        wvaName= GetWavesDataFolder(wva,4)
        wvbName= GetWavesDataFolder(wvb,4)
                if( (CmpStr(wvaName,"")) != 0 %| (CmpStr(wvaName,"")!= 0))
                Abort "Cursors must be on waves"
                return NaN
        endif
        if( CmpStr(wvaName,wvbName))
                Abort "Cursors must be on the same wave (Cursor A is on wave \""+wvaName+"\"; Cursor B
isn't)."
                return NaN
        endif
        Variable p1=pcsr(A)
        Variable p2=pcsr(B)
```

```
	if( p1 > p2 )
		p1=p2
		p2=pcsr(A)
	endif
	Duplicate/O/R=[p1,p2] wva, s_ywave
	WAVE wvx= CsrXWaveRef(A)			// could be non-existant
	if( WaveExists(wvx) )
		Duplicate/O/R=[p1,p2] wvx,s_xwave
		if( IsMonotonicIncrP1P2(s_xwave,0,p2-p1) == 0 )
			Abort "X values between cursors aren't monotonically increasing or decreasing."
			return NaN
		endif
	endif
	Variable x1=hcsr(A)
	Variable x2=hcsr(B)
	if( x1 > x2 )
		x1= x2
		x2=hcsr(A)
	endif
	Variable a
	if( WaveExists(wvx) )
		a= AreaXY(s_xwave,s_ywave,x1,x2)
		Killwaves/Z s_xwave
	else
		a= area(s_ywave,x1,x2)
	endif
	Killwaves/Z s_ywave
	return A
end
Macro Integralberechnung(Untergrundkorrektur)
	string Untergrundkorrektur
	prompt Untergrundkorrektur, "Art der Basislinie?", popup, "x-Achse;durch Cursor mit kleinerem Wert;Verbindung zwischen Cursors"
	PauseUpdate;Silent 1
	Variable/G V_areaXY= fAreaXYBetweenCursors()
	Variable x1=hcsr(A)
	Variable x2=hcsr(B)
	Variable yWert=vcsr(B)
	string Text
	if( x1 > x2 )
		x1= x2
		x2=hcsr(A)
	endif
	if(vcsr(B) > vcsr(A))
		yWert=vcsr(A)
	endif
	if(!cmpstr(Untergrundkorrektur, "x-Achse"))
		Print "FlŠche von", CsrWave(A), "zwischen x =",x1,"und",x2,"=",V_areaXY
		Text="A\\B0\\M("+ CsrWave(A) + "): "
	endif
	if(!cmpstr(Untergrundkorrektur, "durch Cursor mit kleinerem Wert"))
		V_AreaXY -=  yWert/2*(x2-x1)
		Print "FlŠche von", CsrWave(A), "(minus Rechteck) zwischen x =",x1,"und",x2,"=",V_areaXY
		Text="A\\Br\\M("+ CsrWave(A) + "): "
	endif
	if(!cmpstr(Untergrundkorrektur, "Verbindung zwischen Cursors"))
		V_AreaXY -=  (vcsr(A)+vcsr(B))/2*(x2-x1)
		Print "FlŠche von", CsrWave(A), "(minus Trapez) zwischen x =",x1,"und",x2," =",V_areaXY
```

```
		Text="A\\Bt\\M("+ CsrWave(A) + "): "
	endif
	string Welle = CsrWave(A)
	variable Punkt = round(pcsr(A) + pcsr(B))
	Text= Text   + num2str(V_areaXY)
	Tag/O=0/F=0/A=MB/L=0 $Welle, Punkt, Text
End
| IsMonotonicIncrP1P2() returns true if the wave has delta(wave(x))/delta(x) > 0 for all points from p1 to p2.
| p1 must be < p2; these are point numbers, not x values
Function IsMonotonicIncrP1P2(wv,p1,p2)
	Wave wv
	Variable p1,p2
	Variable diff,i=p1
	Variable last=p2
	Variable incr=(wv[p1+1]-wv[p1])>0
	do
		if(incr)
			diff=wv[i+1]-wv[i]
		else
			diff=wv[i]-wv[i+1]
		endif
		if (diff<=0)
			return 0
		endif
		i += 1
	while (i < last)
	return 1
End
```

4.3 CF_3^+ power dependence data

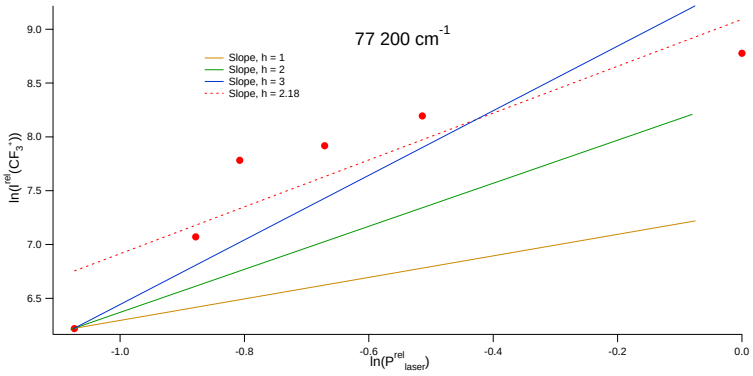

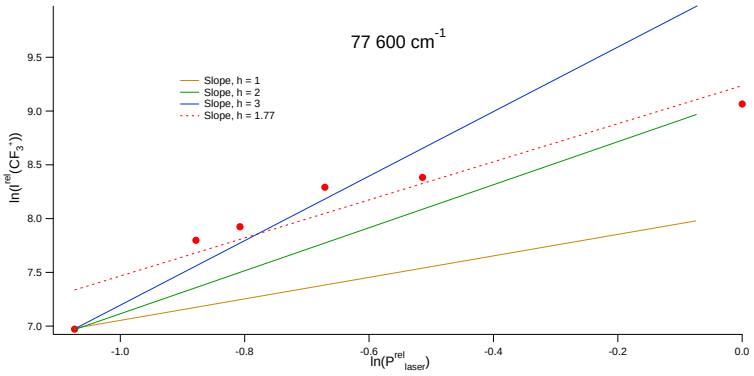

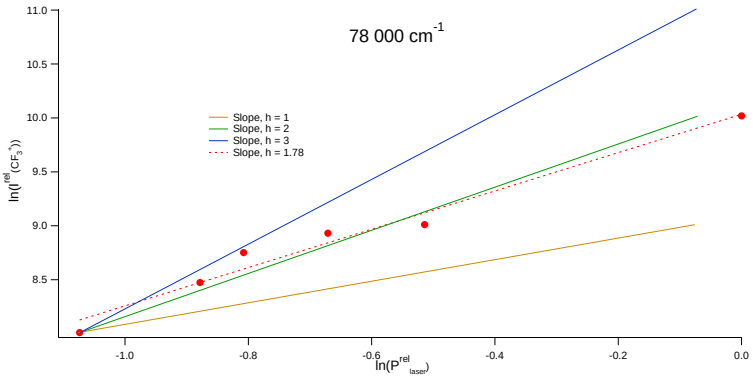

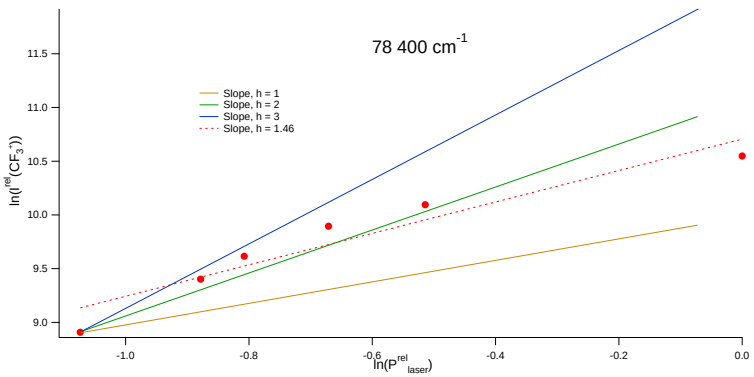

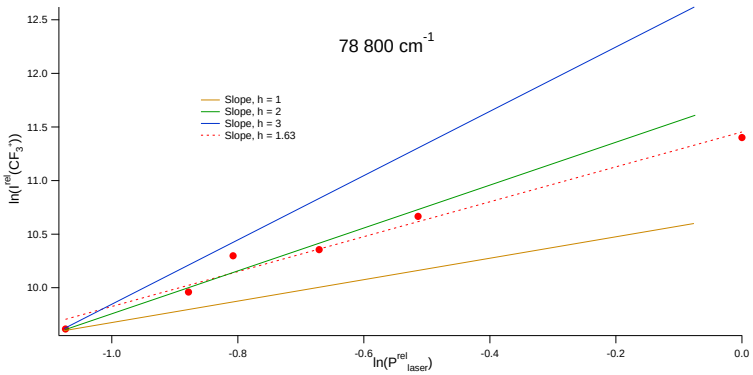

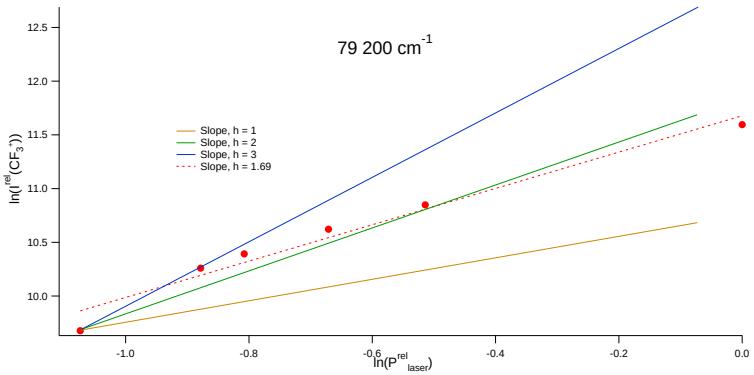

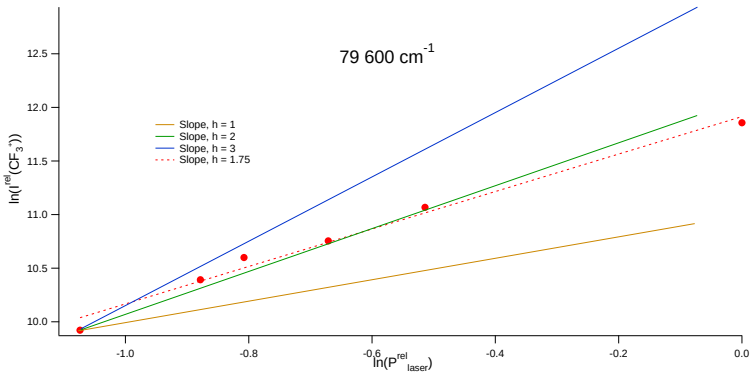

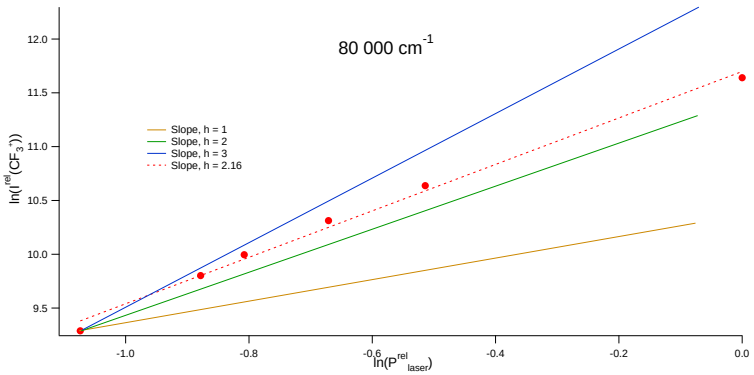

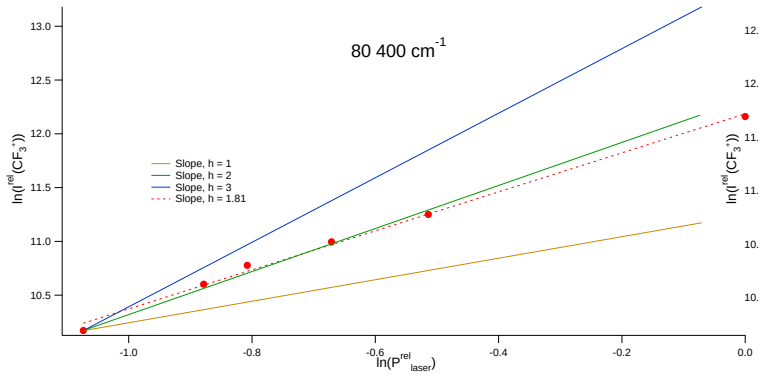
80 400 cm-1
Slope, h = 1
Slope, h = 2
Slope, h = 3
Slope, h = 1.81
ln(I^rel(CF3+))
ln(P^rel laser)

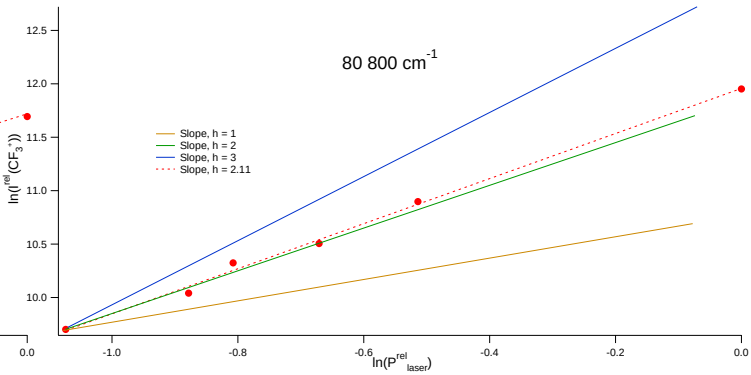
80 800 cm-1
Slope, h = 1
Slope, h = 2
Slope, h = 3
Slope, h = 2.11
ln(I^rel(CF3+))
ln(P^rel laser)

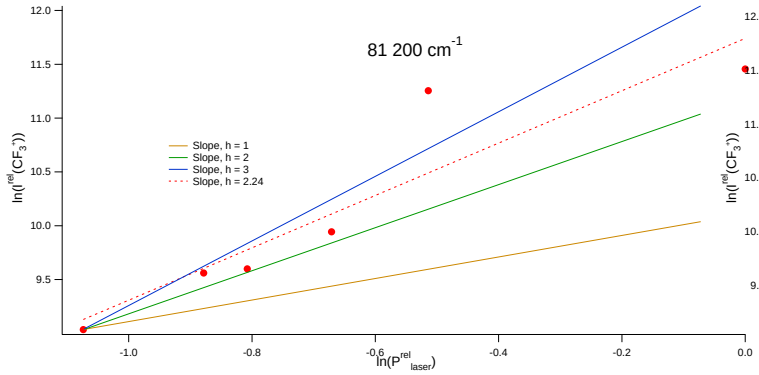
81 200 cm-1
Slope, h = 1
Slope, h = 2
Slope, h = 3
Slope, h = 2.24
ln(I^rel(CF3+))
ln(P^rel laser)

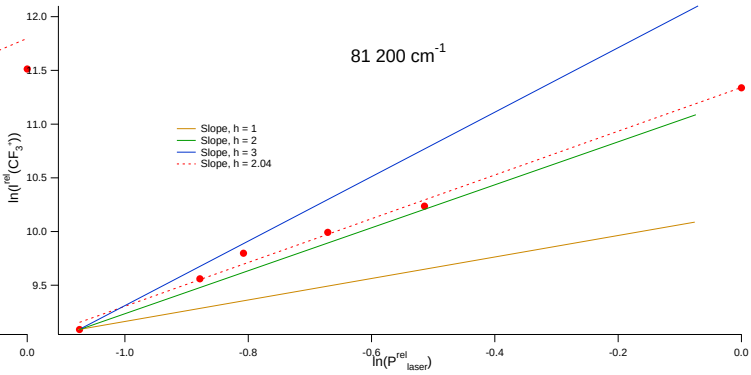
81 200 cm-1
Slope, h = 1
Slope, h = 2
Slope, h = 3
Slope, h = 2.04
ln(I^rel(CF3+))
ln(P^rel laser)

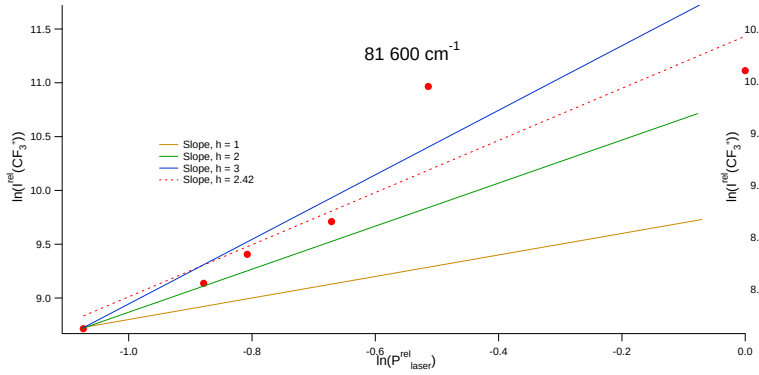
81 600 cm-1
Slope, h = 1
Slope, h = 2
Slope, h = 3
Slope, h = 2.42
ln(I^rel(CF3+))
ln(P^rel laser)

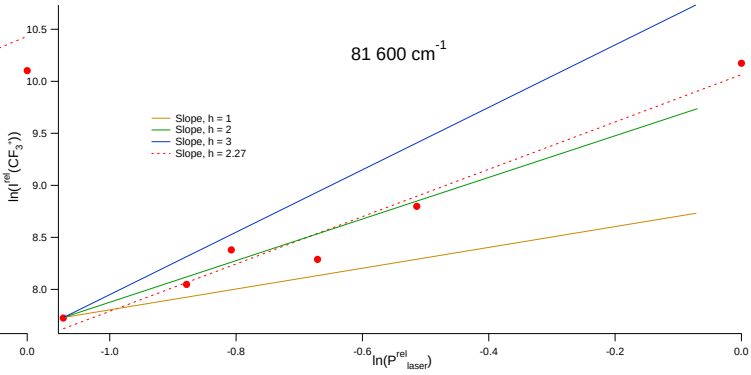
81 600 cm-1
Slope, h = 1
Slope, h = 2
Slope, h = 3
Slope, h = 2.27
ln(I^rel(CF3+))
ln(P^rel laser)